THE PENNSYLVANIA STATE UNIVERSITY
SCHREYER HONORS COLLEGE

DEPARTMENT OF BIOENGINEERING

THE ROLE OF NANOFIBER ARCHITECTURE IN NF-κB SIGNALING

CHRISTOPHER XIGHLUN HONG
Spring 2012

A thesis
submitted in partial fulfillment
of the requirements
for a baccalaureate degree
in Bioengineering
with honors in Bioengineering

Reviewed and approved* by the following:

Peter J. Butler
Associate Professor in Bioengineering
Thesis Supervisor

Justin L. Brown
Assistant Professor in Bioengineering
Honors Adviser

* Signatures are on file in the Schreyer Honors College.

ABSTRACT

The emerging field of tissue engineering and regenerative medicine involves the application of stem cells, biomaterial scaffolds and growth factors either alone or in combination to generate or regenerate damaged or diseased tissue [1]. Previous studies have demonstrated that polymer nanofiber scaffolds provide a suitable environment for mineralized matrix formation and may serve as a substrate for bone tissue growth [2]. In this thesis, we seek to understand the effect of nanofiber substrates on bone growth by studying the regulation of the nuclear factor κ B (NF-κB) signaling pathway. NF-κB is a transcription factor responsible for the regulation of the differentiation and activity of many skeletal cell types, including osteocytes, osteoblasts, osteoclasts, and chondrocytes [3]. Poly(methyl methacrylate) nanofibers of varying diameters and densities were successfully synthesized via electrospinning. MC3T3-E1 Subclone 4 cells were cultured on control and nanofiber substrates for 12, 24 and 48 hours. Two important proteins in the NF-κB pathway, osteoprotegerin (OPG) and the receptor activator for NFκB-ligand (RANKL) were characterized through Western blotting and immunofluorescence assays. Results indicate that electrospun PMMA nanofiber scaffolds encourage a pro-remodeling phenotype in osteoblasts and may be a suitable substrate for bone tissue engineering applications. Through this study, we seek to understand the mechanisms behind osteoblast differentiation on nanofiber scaffolds leading to the engineering of scaffolds in such a way to promote mineralized bone formation [4].

Table of Contents

List of Figures iv
Acknowledgements vi

Chapter 1. Introduction 1

1.1 Bone tissue 1
1.2 Clinical relevance 2
1.3 Bone tissue engineering 2
1.4 Nuclear factor κ B (NFκB) regulation 3
1.5 Significance of research 6
1.6 Hypothesis and specific aims 7

C**hapter 2. MC3T3 Cell Culture on Electrospun Nanofibers** 8

2.1 Background on electrospinning 8
2.2 Experimental methods 9
2.2.1 Electrospinning apparatus 9
2.2.2 Nanofiber synthesis 10
2.2.3 Cover slip preparation 10
2.2.4 Cell line culture 10
2.2.5 Cell seeding 11
2.2.6 Nanofiber characterization 11
2.3 Results 12
2.3.1 Nanofiber synthesis results 12
2.3.2 Cell culture on control and nanofiber substrates results 14
2.4 Discussion 17

Chapter 3. Qantitative and Qualitative Characteration of OPG and RANKL 19

3.1 Background on OPG and RANKL 19
3.2 Experimental methods 19
3.2.1 Cell culture 19
3.2.2 Western blot 19
3.2.3 Immunofluorescence assay 20
3.3 Results 21
3.3.1 Western blot results 21
3.3.2 Immunofluorescence assay results 24
3.4 Discussion 26

Chapter 4. Modulating Nanofiber Diameter and Density 29

4.1 Background on nanofiber modulation 29

4.2 Experimental methods 31
4.2.1 Controlling nanofiber density 31
4.2.2 Controlling nanofiber diameter 31
4.2.3 Assessing nanofiber diameter and density 31
4.3 Results 32
4.3.1 Nanofiber density increases with electrospinning time 32
4.3.2 Nanofiber diameter increases with polymer concentration 35
4.4 Discussion 38

Chapter 5. Conclusions 41

5.1 Summary conclusions 41
5.2 Future work 43

References 44

LIST OF FIGURES

Figure 1.1.1 NF-κB signaling pathway involving OPG, RANK, and RANKL. The effect of this system on bone remodeling is particularly important. Greater ratios of OPG to RANKL lead to osteoclast apoptosis, whereas greater ratios of RANKL to OPG lead to osteoclast proliferation [5].....4

Figure 2.1.1 Basic electrospinning apparatus setup.....8

Figure 2.2.1 Laboratory electrospinning apparatus setup.....9

Figure 2.3.1 PMMA nanofiber substrate on glass cover slip after heating.....12

Figure 2.3.2 Electrospun nanofibers under bright field microscopy at **(A)** 20x and **(B)** 40x magnification 13

Figure 2.3.3. SEM images of PMMA nanofibers at **(A)** 1000x, **(B)** 2500x, **(C)** 5000x and **(D)** 10000x magnification [Tugba Ozdemir] 14

Figure 2.3.4 MC3T3 cells cultured on control and nanofiber substrates for 12, 24 and 48 hours. Cells are stained to identify nucleus (blue) and actin (green) 15

Figure 2.3.5 SEM micrograph of MC3T3 cells proliferating on electrospun nanofibers.....16

Figure 2.3.6 DNA concentrations of cells cultured on control and fiber substrates at 12, 24 and 48 hour time points. Standard error means were used in this analysis with n=3.....17

Figure 3.3.1 Western blot of OPG for control and nanofiber substrates at 12, 24 and 48 time points 21

Figure 3.3.2 Relative optical density of OPG for control and nanofiber substrates at 12, 24 and 48 time points. Optical densities were normalized to the 12 hour control 22

Figure 3.3.3 Western blot of RANKL for control and nanofiber substrates at 12, 24 and 48 time points 22

Figure 3.3.4 Relative optical density of RANKL for control and nanofiber substrates at 12, 24 and 48 time points. Optical densities were normalized to the 12 hour control 23

Figure 3.3.5 Normalized OPG/RANKL ratios 24

Figure 3.3.6 RANKL (green) and OPG (red) expression of a cell on control and nanofiber substrates after 12, 24 and 48 hours 25

Figure 3.3.7 RANKL (green) and OPG (red) expression of a cell on control and nanofiber substrates after 24 hours 26

Figure 4.1.1 Morphology of polyacrylamide nanofibers at varying polymer concentrations [6] 30

Figure 4.3.1. 25% PMMA nanofiber substrates at varying electrospinning durations. Top row left to right: 10, 20 and 30 seconds. Bottom row left to right: 40, 50 and 60 seconds 32

Figure 4.3.2. 25% PMMA nanofibers electrospun for 10, 20, 30, 40, 50 and 60 seconds (A-F, respectively) under a 20X dry objective. Light intensity was increased for D-E 33

Figure 4.3.3. Image of a nanofiber substrate before (left) and after (right) threshold filter 34

Figure 4.3.4. Relative area occupied black pixels after threshold application. The nanofiber substrate spun for 60 seconds was neglected because an accurate threshold could not be obtained due to unfocused fibers. Standard error means were used in the analysis with n=5 35

Figure 4.3.5. Electrospun nanofibers at 10% (A), 15% (B) and 20% (C) PMMA to nitromethane (wt/vol) concentrations. Images were taken using bright field microscopy at 20x magnification 36

Figure 4.3.6. Electrospun nanofibers at 25% (D), 30% (E), 35% (F) and 40% (G) PMMA to nitromethane (wt/vol) concentrations. Images were taken using bright field microscopy at 20x magnification 37

Figure 4.3.7 Nanofiber diameter at varying PMMA polymer concentrations. Standard error means were used in the analysis with n=50 38

ACKNOWLEDGEMENTS

I have been fortunate to meet and work with so many inspiring people throughout undergraduate years at Penn State, many of whom have been invaluable to the completion of this thesis. I would like to thank my research advisor Dr. Justin Brown for his guidance, support and encouragement throughout my project. I would also like to thank my honors advisor, Dr. Peter Butler and my committee member, Dr. Sheereen Majd, for their guidance and critique of my work.

In addition to my professors, there have been other people instrumental to this project. I would like to thank Tugba Ozdemir for teaching and guiding me through many of the laboratory techniques and procedures used in this work. This thesis would not be possible without her direct support, encouragement and assistance. I would also like to thank Razieh Farzad for the use of her cells and Andrew Higgins for his advice on nanofiber synthesis.

Finally, I would like to thank my family and friends for their persistent love and encouragement throughout my complete of this thesis. I would especially like to thank my parents, who have little understanding of NF-κB signaling, but have offered me comfort, motivation and inspiration through every failure, as well as every success.

Chapter 1

INTRODUCTION

1.1 Bone tissue

Bone is a dynamic, vascularized tissue that possesses the unique ability to remodel continuously [7]. As a major tissue comprising the skeleton, its primary purpose is to provide mechanical support and structural framework for the body. Due to its mineralized matrix, bone has an exceptionally high elastic modulus, compressive strength and toughness compared to other body tissues. In addition, bone serves as a mineral reservoir for calcium and has the ability to quickly activate mineral stores based on metabolic demand, as predominantly regulated by parathyroid hormone [7], [8].

Bone tissue formation and resorption is regulated by complex cellular and molecular communication between bone cells. Osteoblasts differentiate from mensenchymal stem cells and are responsible for secreting an organic osteoid matrix which promotes mineralized hydroxyapatite formation from nucleation of calcium and phosphate on deposited type I collagen [9], [10]. When osteoblasts are surrounded by bone, they either undergo apoptosis or differentiate into osteocytes, which maintain cellular communication and respond to mechanical forces. On the other hand, osteoclasts play an important role in bone remodeling by resorbing both organic and inorganic components of bone. Osteoclasts resorb bone by attaching onto the surface and secreting acid proteases. These enzymes aid mineral solubilization and organic matrix digestion. The delicate balance between bone deposition and resorption is integral to maintaining proper bone integrity [8]. Disturbances in this equilibrium are responsible for the

development of numerous human diseases, inducing osteoporosis, Paget's disease, and rheumatoid arthritis [10].

1.2 Clinical relevance

Every year, roughly 1 million cases of skeletal defects require bone-graft treatments. Bone grafts are often used to provide mechanical support, fill voids, and promote repair of damaged bone tissue [11]. Current methods of replacing and repairing damaged bone tissue include using autografts, allografts and synthetic biomaterials. However, these approaches are hindered by multiple problems: autografts are expensive and often lead to complications after the procedure; allografts exhibit immunocompatability difficulties and poor mechanical properties; synthetic biomaterials cannot mimic the mechanical properties of bone and intrinsically lack the ability to promote *de novo* bone formation [12]. Metals and ceramics have served as a substitute for bone grafts. However, neither is ideal as a permanent solution; metals do not integrate well with tissue at the implantation site and can fail because of infection or fatigue loading, and ceramics exhibit very low tensile strength, thus rendering them incapable of experiencing significant torsion, bending, or shear stress [7].

1.3 Bone tissue engineering

Tissue-engineered bone, created by growing precursor bone cells on a biocompatible 3-D scaffold, is a potential bone graft substitute that can mimic the mechanical and structural properties of bone and exhibit biological and immunological compatibility [1], [12]. These promising cell-based tissue scaffold constructs can be grown outside the body then grafted back into the host to promote bone regeneration [13]. Transplanted cells are expected to secrete new growth factors and matrix proteins while the polymer gradually degrades. Appropriate scaffolds need to possess several essential properties: biocompatility, porosity, proper pore size, proper

surface properties, and osteoconductivity and osteoinductivity [1], [7]. Highly porous scaffolds are ideal to accommodate a large number of cells and facilitate gas and nutrient diffusion [14]. Osteoconductivity, the ability to support the growth of new osteoblasts and osteoprogenitor cells, and osteoinductivity, the ability to promote osteoblastic differentiation of progenitor cells, are especially important design parameters. Although cell-based tissue scaffolds have much promise, current efforts at synthesizing a bone-like matrix in vitro have been unsuccessful in generating the volume of bone matrix necessary for implantation [13].

Artificially engineered nanofibers serve as a potential substrate that may promote bone matrix formation for bone tissue engineering. Many types of nanofibers play important roles in the body. For instance, collagen fibers comprise the extracellular matrix of bone, cartilage, and blood vessel tissues, among others [15]. Engineered polymer nanofibers can mimic the mechanical properties of extracellular matrix and can be used for tissue engineering applications [2], [15], [16]. Many different types of biocompatible polymers have been used for tissue engineering applications, including sodium alginate/poly(ethylene oxide), poly(methyl methacrylate) and polyphosphazine/hydroxyapatite [16–18]. Polymer electrospun nanofibers also exhibit high specific surface area with excellent pore interconnection, making them ideal for tissue engineering applications [15]. In this study, we look to determine the effect of nanofiber substrates on the NF-kB signaling pathway in osteoblasts.

1.4 Nuclear factor κ B (NFκB) regulation

Nuclear factor kappa-light-chain-enhancer of activated B cells (NF-κB) is a family of transcription factors that controls the activity or differentiation of several skeletal cell types, but primarily the differentiation of osteoclasts from hematopoietic stem cells [9]. The NF-κB pathway is activated during embryogenesis and has been shown to affect endochondral

ossification [3]. Furthermore, previous studies have shown that the pathway plays a role in a number of skeletal diseases and conditions, including postmenopausal osteoporosis, Paget's disease, inflammatory response, osteoarthritis, and metastatic bone diseases [19].

The initiation of osteoclastic demineralization begins with the binding of the receptor activator for NFκB-ligand (RANKL), a membrane bound ligand expressed by osteoblasts in a mechanically quiescent environment, to the RANK receptor on the surface of the hematopoietic stem cells [20–22]. This binding triggers a cascade of intracellular processes, including the translocation of NF-κB to the pre-osteoclast nucleus, and results in the differentiation of the pre-osteoclast into a mature osteoclast. Overall, this leads to increased bone resorption. The binding of RANK to RANKL is regulated by osteoprotegerin (OPG), a competitive receptor to RANK that is expressed by mature osteoblasts producing osteoid matrix in response to a mechanical stimulus [3]. A schematic of this process is illustrated in Figure 1.1.1.

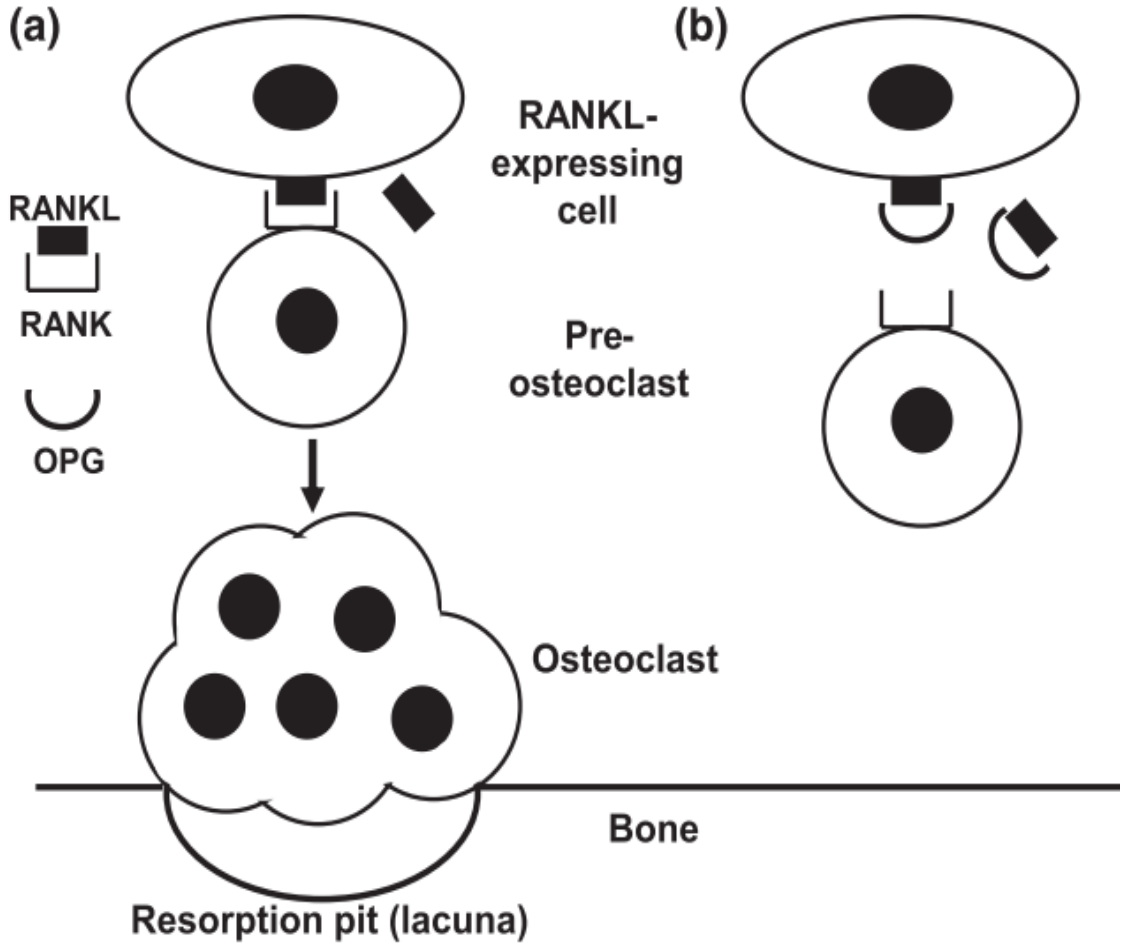

Figure 1.1.1 NF-κB signaling pathway involving OPG, RANK, and RANKL. The effect of this system on bone remodeling is particularly important. Greater ratios of OPG to RANKL lead to osteoclast apoptosis, whereas greater ratios of RANKL to OPG lead to osteoclast proliferation [5], [10].

Recent studies have indicated that the expression of RANKL and OPG is directly correlated to the degree of bone differentiation [5]. By understanding the effects of nanofiber substrates on the expression of these proteins, nanofibers can be constructed in such a way that promotes the expression of OPG while suppressing the expression of RANKL, thereby enhancing the development of mineralized tissue.

1.5 Significance of research

The mechanical and dimensional properties of the extracellular matrix are well known regulators of cell proliferation and differentiation [4]. Nevertheless, the complex signaling mechanisms leading to cellular response remain largely unknown [9]. In this study, we seek to understand the efficacy of tissue engineered nanofiber substrates on osteoblast regulation of (NF-κB), an important signaling protein in osteoclast formation, and its effect on the development of *de novo* bone tissue formation.

By understanding the cellular response of osteoblasts on nanofibers, nano-scaffolds can be engineered in such a way to elicit the formation of a mineralized matrix and inhibit the resorption of the newly forming mineralized matrix.

1.6 Innovation of research

Currently, no studies have been conducted on the NF-κB signaling of osteoblasts on nano-scaffolds. This study builds upon previous research concerning osteoblasts growing under fluid shear stress. It has been demonstrated that unidirectional fluid shear stress applied to osteoblasts stimulates production of RANKL [4]. However, pulsatile fluid shear stress inhibits production of RANKL while promoting production of OPG [12]. While it remains unclear why cells respond differently to varying forms of fluid shear, we observe that unidirectional fluid shear imposes a general steady-state effect, while pulsatile fluid shear stress produces unsteady and time-variant changes. This concept can be applied to osteoblast proliferation on different substrates. A flat polymer substrate provides a “steady-state” surface for cell growth; osteoblasts proliferate in all directions without major constraints. However, osteoblasts growing on a nanofiber substrate encounter mechanical discontinuities related to adhesion and migration along nanofibers (similar to how a tight-rope walker constantly flexes and relaxes his muscles to

maintain balance); the cellular cytoskeleton must constantly adjust in this "unsteady" environment as a cell migrates and proliferates [23]. To our knowledge, this is the first study to recreate the dynamic culture properties through static nanofiber substrates and observe the effect of nanofiber substrates on osteocyte proliferation through NF-κB signaling.

1.7 Hypothesis and specific aims

We hypothesize that electrospun nanofiber scaffolds will promote osteoblastic differentiation and mineralized bone formation due to inhibition of NF-κB activation. Furthermore, the degree of osteoblastic differentiation will differ between nanofibers of varying diameters and densities; these parameters can be optimized for maximal bone growth.

Specific Aim 1: To synthesize poly(methyl methacrylate) (PMMA) nanofibers via electrospinning and culture MC3T3 osteoblast on the nanofiber substrates. Specific Aim 1 will be considered a success if nanofibers around 1μm are spun without significant spraying or beading and osteoblasts are able to proliferate on the nanofiber subsubstrates.

Specific Aim 2: To qualitatively and quantitatively determine the expression of OPG and RANKL of osteocytes on control and nanofiber substrates at 1, 12, 24, and 48 hour time points. Specific Aim 2 will be considered a success if Western blotting and immunofluorescence assays reveal altered expression and localization between control and nanofiber substrates.

Specific Aim 3: To electrospin PMMA nanofibers of varying diameters and densities by modifying polymer concentration and electrospinning time, respectively. Specific Aim 3 will be considered a success if nanofibers substrates of varying diameter and density are synthesized.

Chapter 2

MC3T3 CELL CULTURE ON ELECTROSPUN NANOFIBERS

2.1 Background on electrospinning

Nanofibers can be synthesized from a wide range of polymer using various methods, including template, self-assembly, phase separation, melt-blow, and electrospinning [15]. Recently, electrospinning is being actively explored due to its simplicity, cost-effectiveness, and usefulness in producing ultrafine nanofibers with high specific surface areas and high porosities [14], [16]. In electrospinning, a high voltage charges a viscous polymer solution. The electrostatic forces draw the solution into a liquid jet that forms solid fibers upon solvent evaporation. The basic equipment used in electrospinning is shown in Figure 2.1.1.

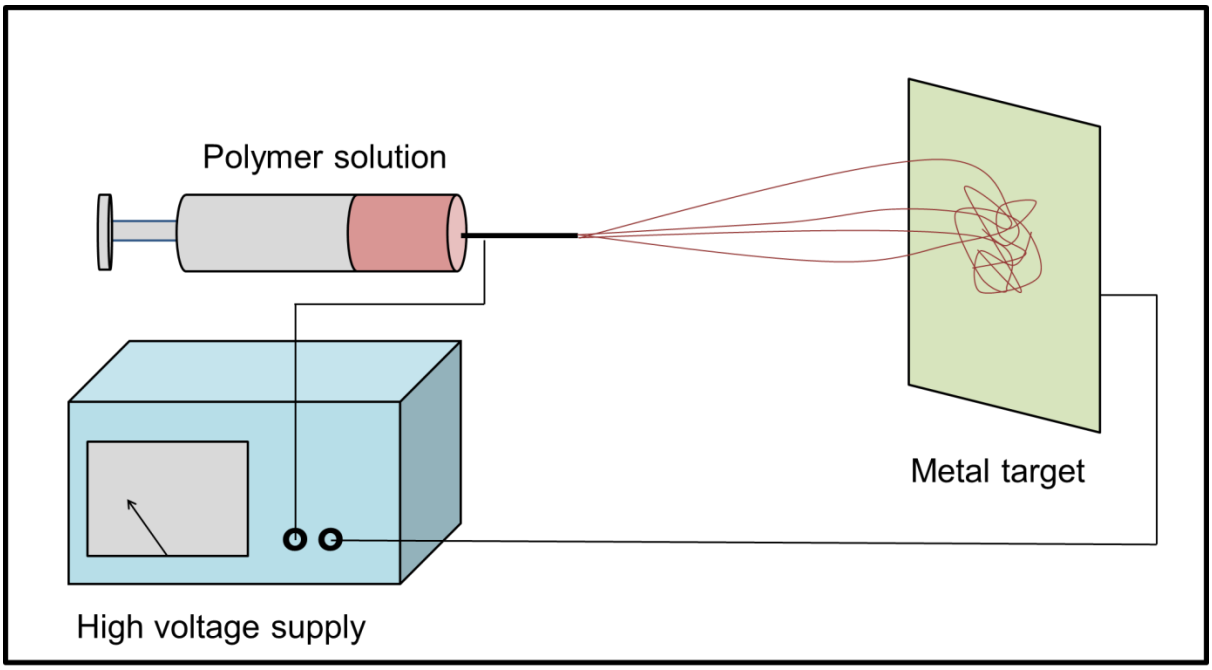

Figure 2.1.1 Basic electrospinning apparatus setup. A high voltage source is connected to the tip of the needle and a metal target. The polymer feed rate is regulated by a pump (not pictured).

In the present study, we explored the use of PMMA as a polymer for electrospinning. PMMA, an amorphous polymer, is a biocompatible polymer commonly used as bone cements and intraocular lenses [24]. Previous studies have indicated that PMMA is capable of forming a wide range of nanofiber morphologies and supporting cell growth [25]. We also explored the viability of culturing preosteoblast cells on PMMA nanofiber substrates.

2.2 Experimental methods

2.1.1 Electrospinning apparatus

All the equipment for the electrospinning apparatus, apart from the voltage source, was contained inside a clear acrylic box. The equipment position and orientation are shown in Figure 2.2.1.

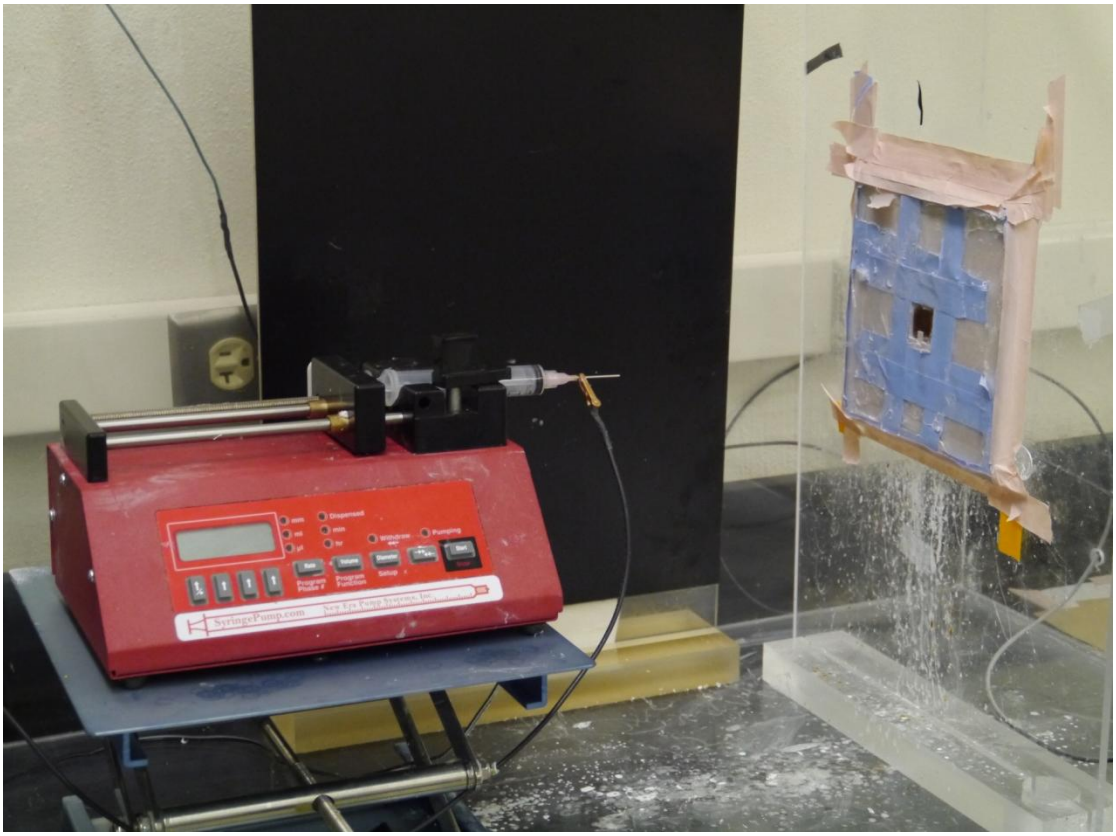

Figure 2.2.1 Laboratory electrospinning apparatus setup. A needle was placed in the syringe pump (red object). An alligator clip connected the tip of the needle to the voltage

source (not pictured). The voltage source was also connected to the metal target via wire. The metal target exhibited a small exposed area at its center. This promoted polymer deposition at the target's center, where the cover slip was placed.

2.2.2 Nanofiber synthesis

Poly(2-hydroxyethyl methacrylate) (PolyHEMA, M_w 20,000) was dissolved in 70% ethanol to produce a 2% PolyHEMA (wt/vol) liquid solution that was spin-coated (3500rpm, 15 s) onto glass cover slips (22x22 mm). PolyHEMA, a biocompatible polymer used as additives in dental resins, was used to restrict cell adhesion to the nanofibers. Poly(methyl methacrylate) (PMMA, M_w 120,000) was dissolved in nitromethane to produce a 25% PMMA (wt/vol) working fluid. The solution was drawn into a plastic syringe through a metallic needle (18 G). The PolyHEMA coated cover slips was attached onto a metal counter-electrode placed 20 cm from the tip of the needle. A high voltage source was connected between the needle and counter-electrode, and a voltage of 10kV was applied. The feed rate of the solution was controlled by a syringe pump. Fibers were spun for 20 seconds. The control group comprised of PolyHEMA cover slips spin-coated (3500rpm, 15 s) with 2% PMMA in nitromethane (wt/vol).

2.2.3 Cover slip preparation

Following nanofiber synthesis, the coated glass cover slips were heated on a hotplate on top of a Kimtech wipe at 200°C for 20 seconds. All cover slips were sterilized under ultraviolet light overnight.

2.2.4 Cell line culture

MC3T3-E1 Subclone 4 cells (ATCC, Manasas, VA) were cultured in 15cm plasma-treated polystyrene petri dishes (Thermo Scientific) under standard culture

conditions (37°C, 95% air/5% CO_2). Cell media (αMEM, Life Technologies) was supplemented with 10% vol/vol fetal bovine serum (FBS; Altanta Biologicals) and 1% vol/vol penicillin streptomycin. Cells were analyzed for confluence through bright field microscopy. When 80-90% confluent, media from the cell culture was aspirated and the cells were washed once with PBS. The cells were detached using trypsin (Life technologies); Trypsin was added to the cells and the dish was placed in an incubator for 5 minutes. The cells were spilt between multiple dishes, and fresh media was introduced back into the dishes.

2.2.5 Cell seeding

Sterilized cover slips were each placed in an individual well in 6-well plates. 1mL of mineralizing media (αMEM, 10% FBS, 1% pen/strep, 3mM β-glycerol phosphate, 10μg/mL ascorbic acid) was introduced to each well to allow protein adsorption prior to seeding. 80-90% confluent MC3T3 cells were washed once with PBS and detached with trypsin. The cells were pelleted and re-suspended in mineralizing media. After, cells were seeded onto the prepared glass slides at 50-60% confluence. Cells were cultured under standard conditions for 12, 24 and 48 hours.

2.2.6 Nanofiber characterization

Nanofibers were imaged through bright field and scanning electron microscopy. Cells were imaged through fluorescence microscopy with the same preparation methods outlined in Methods 3.2.3.

2.3 Results

2.3.1 Nanofiber synthesis results

Nanofibers were successfully electrospun from a 25% wt/vol PMMA solution. Macroscopically, the substrate appears as a thin white sheet, as seen in Figure 2.3.1. Bright field microscopy shows that the nanofibers overlap to form a homogeneous polymer network with little beading, as shown in Figure 2.3.2. Nanofiber diamaters were characterized using ImageJ software and found to have a mean of 1.50μm with a standard deviation of 0.21μm.

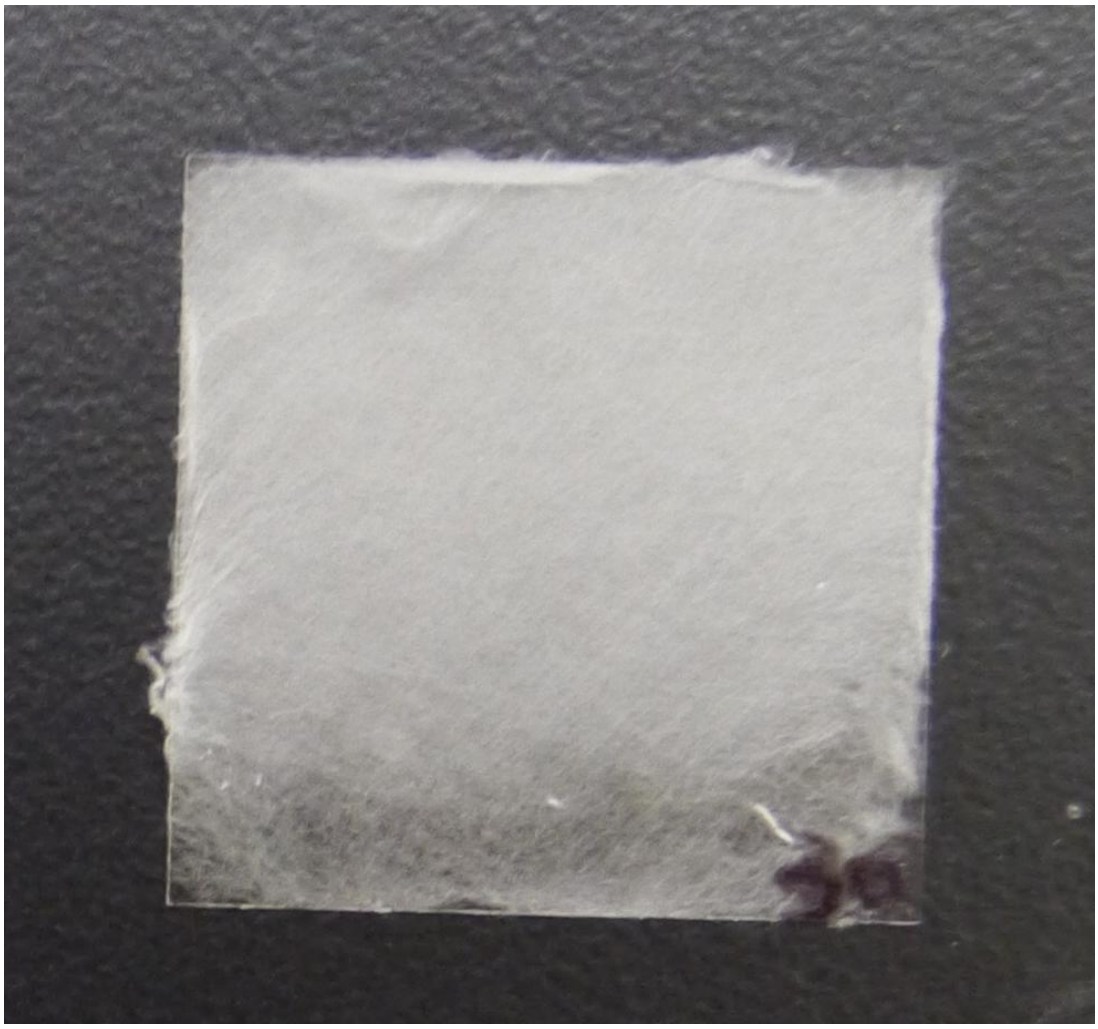

Figure 2.3.1 PMMA nanofiber substrate on glass cover slip after heating.

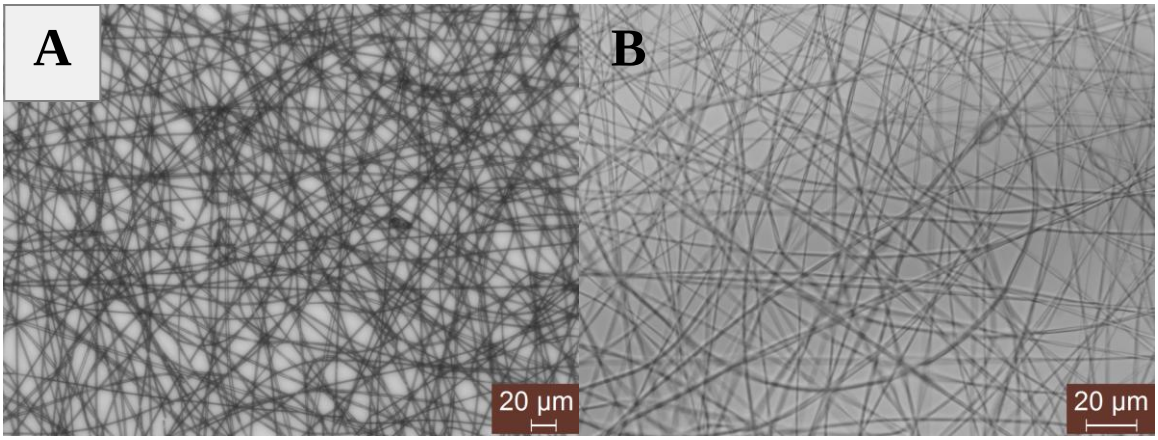

Figure 2.3.2 Electrospun nanofibers under bright field microscopy at **(A)** 20x and **(B)** 40x magnification.

As shown in Figure 2.3.3, SEM micrographs of PMMA nanofibers synthesized through a similar method reveal a homogeneous network of relatively uniform nanofibers. The small clumps observed on the fibers are due to polymer beading.

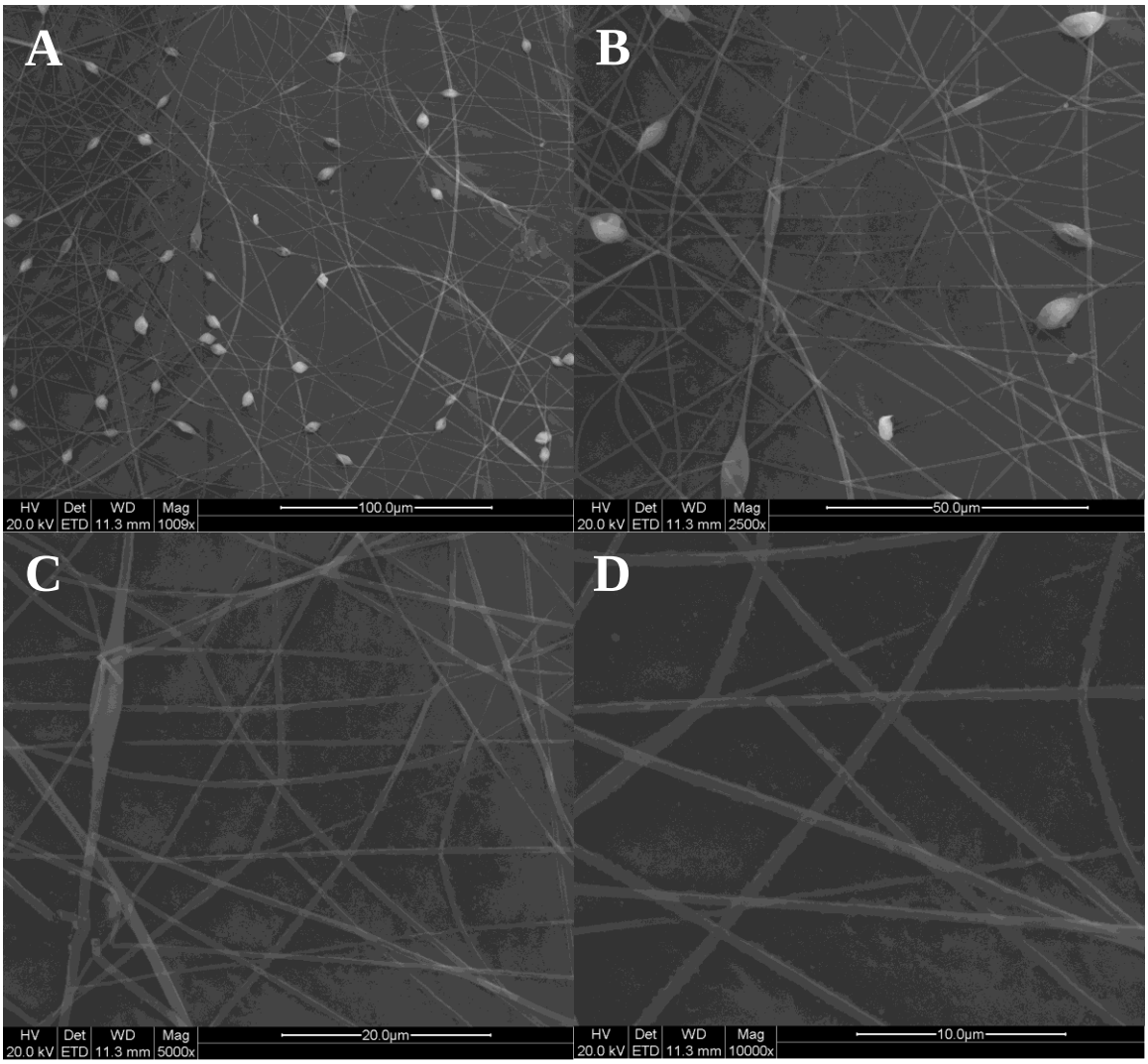

Figure 2.3.3. SEM images of PMMA nanofibers at **(A)** 1000x, **(B)** 2500x, **(C)** 5000x and **(D)** 10000x magnification. (Tugba Ozdemir).

2.3.2 Cell culture on control and nanofiber substrates results

Florescence microscopy confirmed MC3T3 proliferation on both control and nanofiber substrates, as seen in Figure 2.3.4. Actin, a major cytoskeletal protein, was stained to reveal the cells' structural network. For cells growing on control substrates, the cytoskeletal network extends in all directions. For cells growing on nanofiber substrates, the cytoskeleton extends in the direction of local nanofibers.

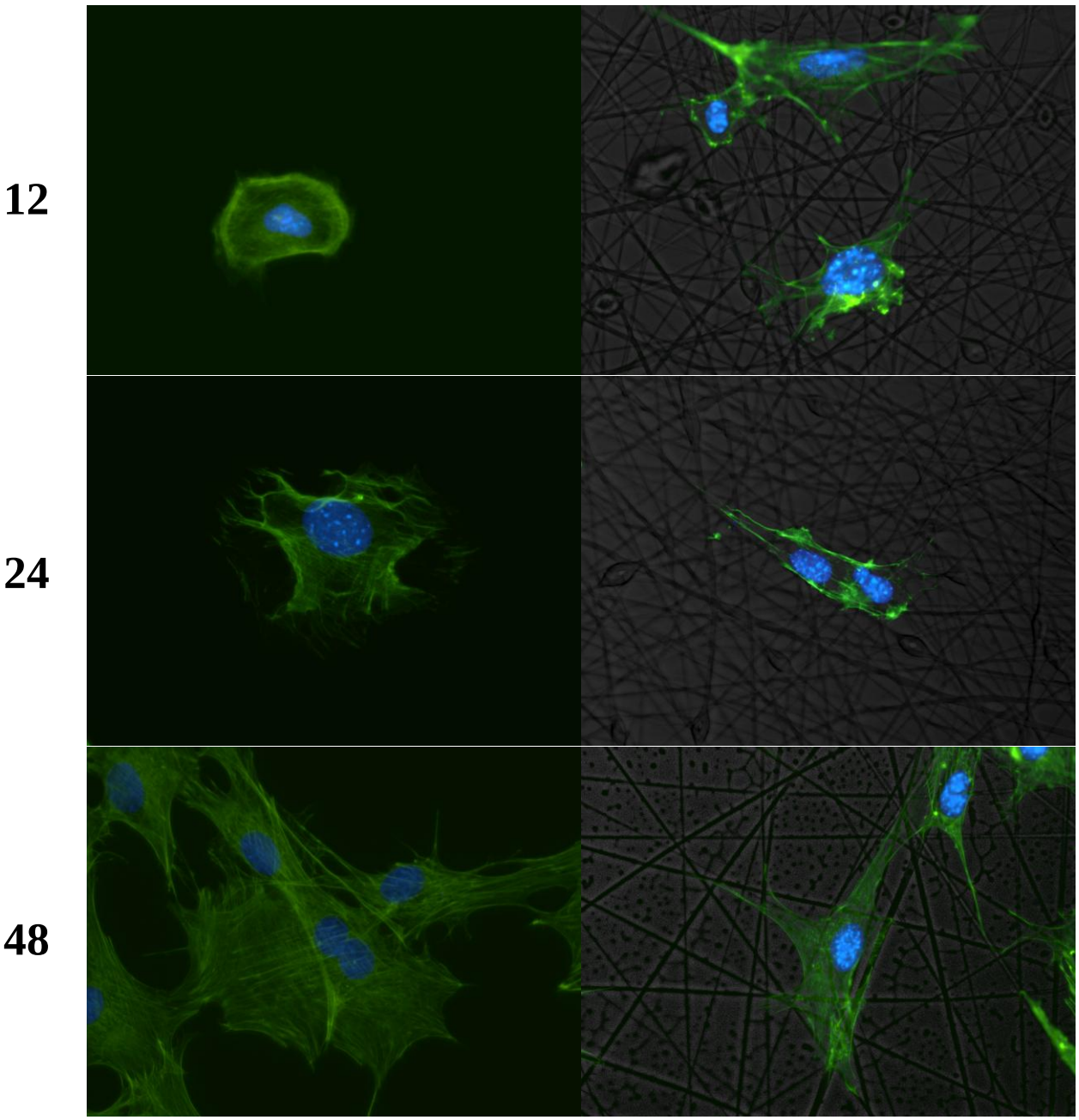

Figure 2.3.4 MC3T3 cells cultured on control and nanofiber substrates for 12, 24 and 48 hours. Cells are stained to identify nucleus (blue) and actin (green).

Electron micrographs of cells on nanofibers scaffolds reveal cellular adhesion to the nanofibers, as seen in Figure 2.3.5. This was expected, since adhesion proteins must

attach to the PMMA substrate for cell movement and proliferation. The polyHEMA coating prevents cells from adhering to the glass surface and forces cells to adhere to the nanofibers.

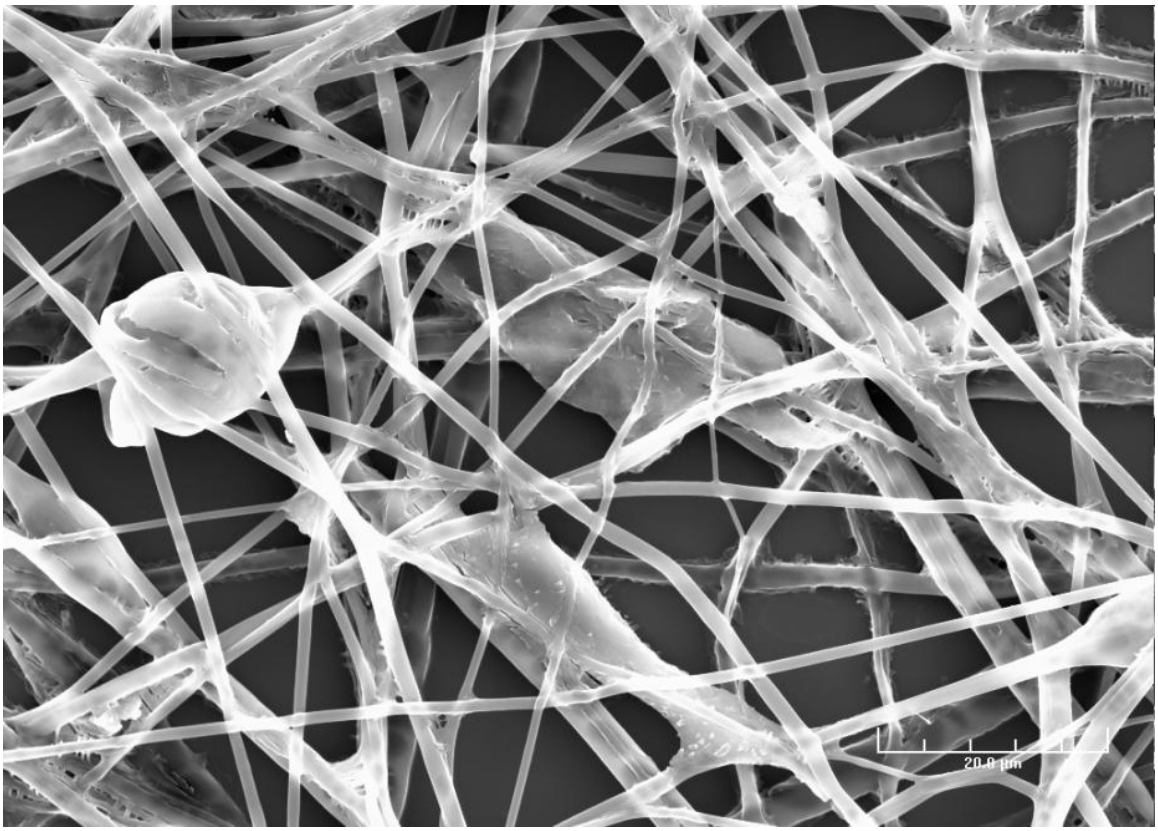

Figure 2.3.5 SEM micrograph of MC3T3 cells proliferating on electrospun nanofibers

DNA concentrations were measured for control and nanofiber substrates at all three time points. As illustrated in Figure 2.3.6, DNA concentration rises for both substrates as culture time increases. At each time point, the DNA concentration was found to be greater for cells on control substrates, although more trials are needed to establish statistical significance.

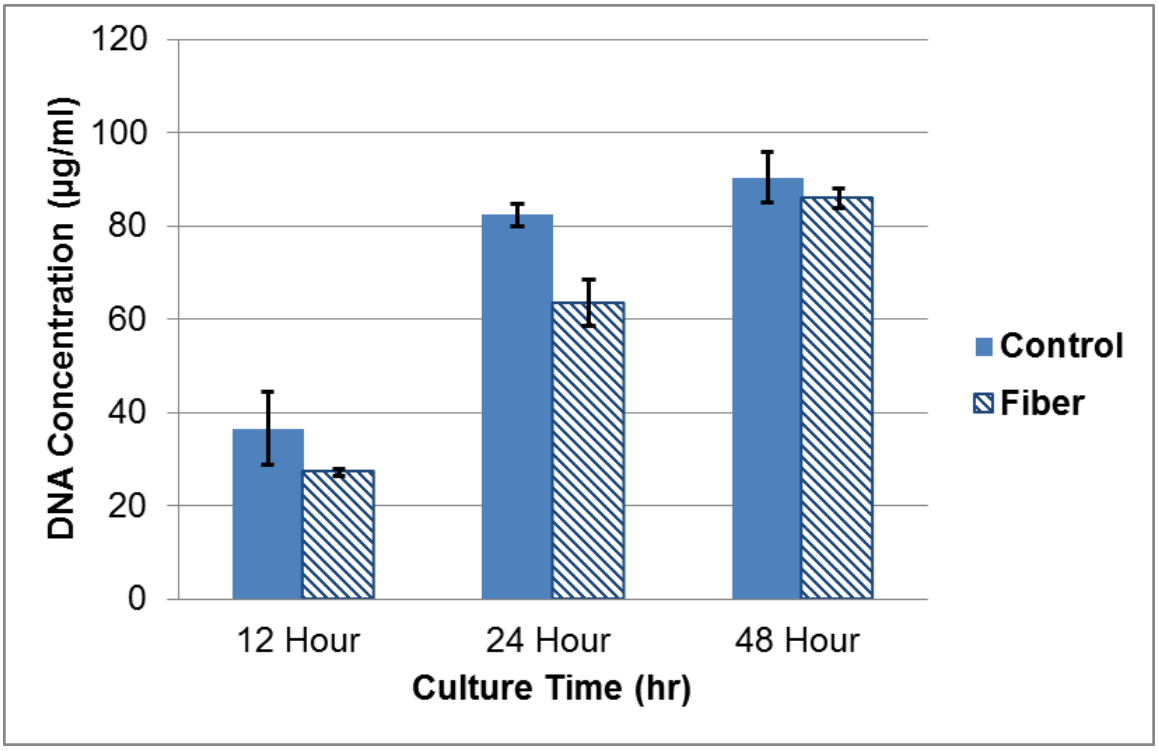

Figure 2.3.6 DNA concentrations of cells cultured on control and fiber substrates at 12, 24 and 48 hour time points. Standard error means were used in this analysis with n=3.

2.4 Discussion

As illustrated in the results, electrospun PMMA nanofibers serve as a suitable substrate for MC3T3 cell culture. PMMA nanofibers were successfully synthesized through electrospinning. Although the nanofiber diameters are not on a nanometer scale, their dimensions are appropriate for cell adhesion. In addition, the fibers were qualitatively observed to have relatively uniform diameter and density across the glass cover slip. This promotes homogenous cell growth across the substrate and suggests uniform tissue distribution in macroscopic applications.

On nanofiber substrates, cells were observed to proliferate in line with the nanofibers, as illustrated in Figure 2.3.4. The cytoskeleton can only extend where integrins can adhere. This supports the hypothesis that cells must constantly adjust to the "unsteady" environment created by the nanofibers as they migrate and proliferate.

Figure 2.3.6 shows the DNA concentration of the cells at the designated time points. The increase in DNA concentration with culture time for both substrates can be attributed to cellular division. Lower DNA concentration on nanofiber substrates suggests that cells on nanofibers divide at a slower rate than cells on control substrates. This may be due to increased osteoid matrix formation induced by the nanofiber substrates; instead of spreading and dividing, cells on nanofiber substrates appear more likely to form mineralized matrix, indicative of osteoblastic differentiation.

This study suggests that PMMA nanofiber scaffolds serve as an osteoconductive substrate that can elicit the formation of a mineralized matrix. Additional research concerning the formation of mineralized matrix should be performed at extended time points. Additional fluorescence assays could stain for cytoskeletal proteins such as vinculin and FAK to gain a better picture of nanofibers affect on cellular cytoskeletal network.

Chapter 3

QUANTITATIVE AND QUALITATIVE CHARACTERATION OF OPG AND RANKL

3.1 Background on OPG and RANKL

The NF-κB signaling pathway plays a large role in regulating osteoclast differentiation. OPG and RANKL are two important proteins involved in this process. High levels of OPG are associated with osteoblastic proliferation and mineralized matrix formation, while high levels of RANKL lead to osteoclastic proliferation and mineralized matrix degradation. In this study, we seek to quantitatively and qualitatively characterize OPG and RANKL protein levels in MC3T3 cells growing on nanofiber substrates. Western blotting is a well-established technique used to qualitatively determine protein concentrations within a cell. In this study, Western blotting was used to characterize levels of OPG and RANKL present in cells growing on control and nanofiber substrates. Furthermore, immunofluorescence assays was performed to determine the localization of OPG and RANKL in the cells.

3.2 Experimental methods

3.2.1 Cell culture

MC3T3 osteoblast cells were seeded on control and nanofiber substrates and grown in standard culture conditions for 12, 24 and 48 hours, as described in section 2.2 Methods.

3.2.2 Western blot

RANKL and OPG were characterized through Western blotting. Grown cells were washed with PBS then lysed using 200µL of low-UV RIPA lysis buffer (150mM

NaCl, 1% Tween20, 0.5% Na deoxycholate, 0.1% SDS, 50mM Tris, pH 8.0, 1:1000 protease inhibitors). DNA concentrations were determined for each sample to normalize the amount of protein loaded in each well. 2µg of DNA from each sample was mixed with a loading buffer and heated at 95°C for 10 minutes prior to loading. A 12% acrylamide/bis-acrylamide (wt/vol) gel (1.5M Tris, 10% SDS, 10% ammonium persulfate, TEMED) was cast and allowed to polymerize. Samples were loaded and the gel was run at 120V for 2.5 hours. Next, the proteins were transferred to a PVDF membrane by applying a voltage of 80V for 80 minutes. The membrane was blocked with 1:1 blocking buffer and TBS for 1 hour, then incubated with primary RANKL and OPG antibodies (1:1000) overnight at 4°C. After three washes with TBST and one wash with TBS, the membrane was incubated with secondary antibodies overnight at 4°C. Antibody binding was detected using infrared fluorescence imaging. Images were taken using Licor Odyssey and data was analyzed using ImageJ software to determine statistical significance.

3.2.3 Immunofluorescence assay

Cells were washed with PBS, then incubated with fixation buffer (3.7% paraformaldehyde in 1X PBS, vol/vol) for 15 minutes. Cells were then washed three times with PBS and incubated with a permeabilization buffer (1X PBS, 2 vol % bovine serum albumin, 0.1 vol % Triton X-100) for 45 minutes. Primary antibodies (1:100 in PB, Santa Cruz Biotechnology) were added and cells were incubated for 1 hour. After washing (PBS, 3x), secondary antibodies (1:200 in PB) were added and cells were incubated for 45 minutes. After washing (PBS, 3x), cells were stained with phalloidin (1:1000 in PB). Cells were washed again (PBS, 3x) and stained with dapi (1:10000 in

PB). After a final set of three washes (PBS, 3x), cover slips were allowed to dry under darkness. When dry, the slides were mounted to glass slides with Profade Gold mounting media and analyzed through fluorescence microscopy.

3.3 Results

3.3.1 Western blot results

Relative protein concentrations for OPG and RANKL were quantified. OPG concentration decreased with time for both control and nanofiber substrates, as seen in Figures 3.3.1 and 3.3.2. OPG expression was greater for the control substrate for the 12 and 24 hour time points, but became greater for the nanofiber substrate at the 48 hour time point.

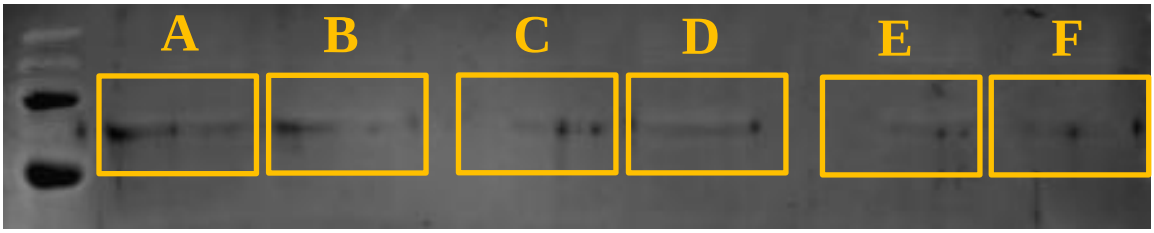

Figure 3.3.1 Western blot of OPG for control and nanofiber substrates at 12, 24 and 48 hour time points. **(A)** 12 hour control and **(B)** nanofiber, **(C)** 24 control and **(D)** nanofiber, and **(E)** 48 control and **(F)** nanofiber.

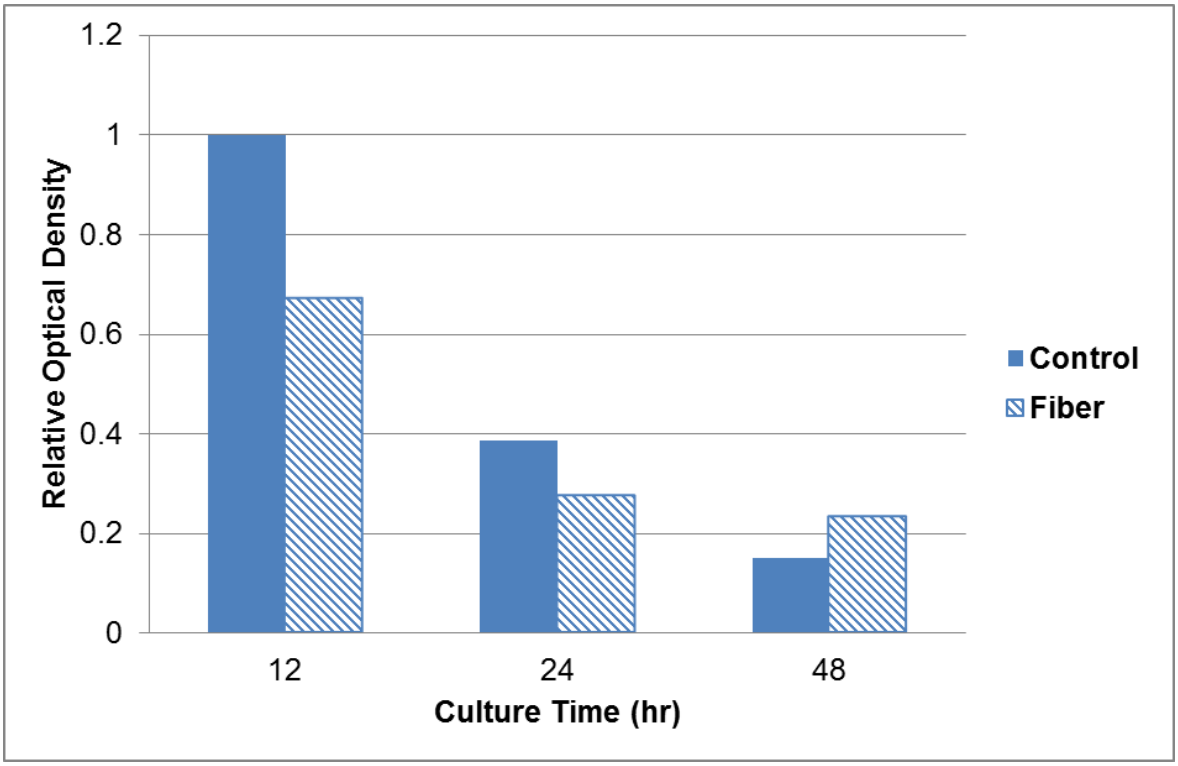

Figure 3.3.2 Relative optical density of OPG for control and nanofiber substrates at 12, 24 and 48 time points. Optical densities were normalized to the 12 hour control.

RANKL expression was noticeably less for control substrates, remaining around the same concentration at all three time points, as seen in Figures 3.3.3 and 3.3.4. RANKL expression for the nanofiber substrate greatly decreased between the 12 and 24 hour time points.

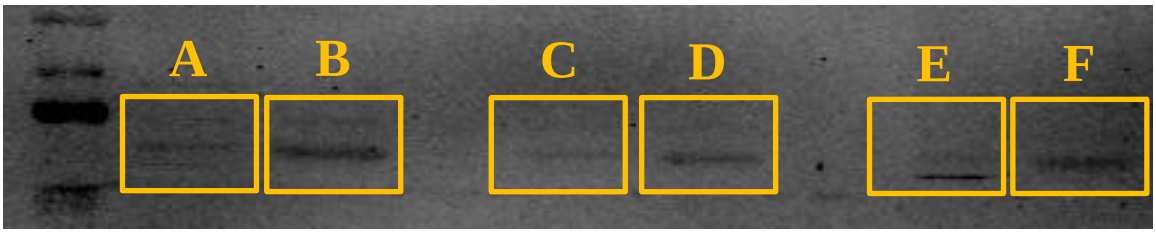

Figure 3.3.3 Western blot of RANKL for control and nanofiber substrates at 12, 24 and 48 hour time points. **(A)** 12 hour control and **(B)** nanofiber, **(C)** 24 control and **(D)** nanofiber, and **(E)** 48 control and **(F)** nanofiber.

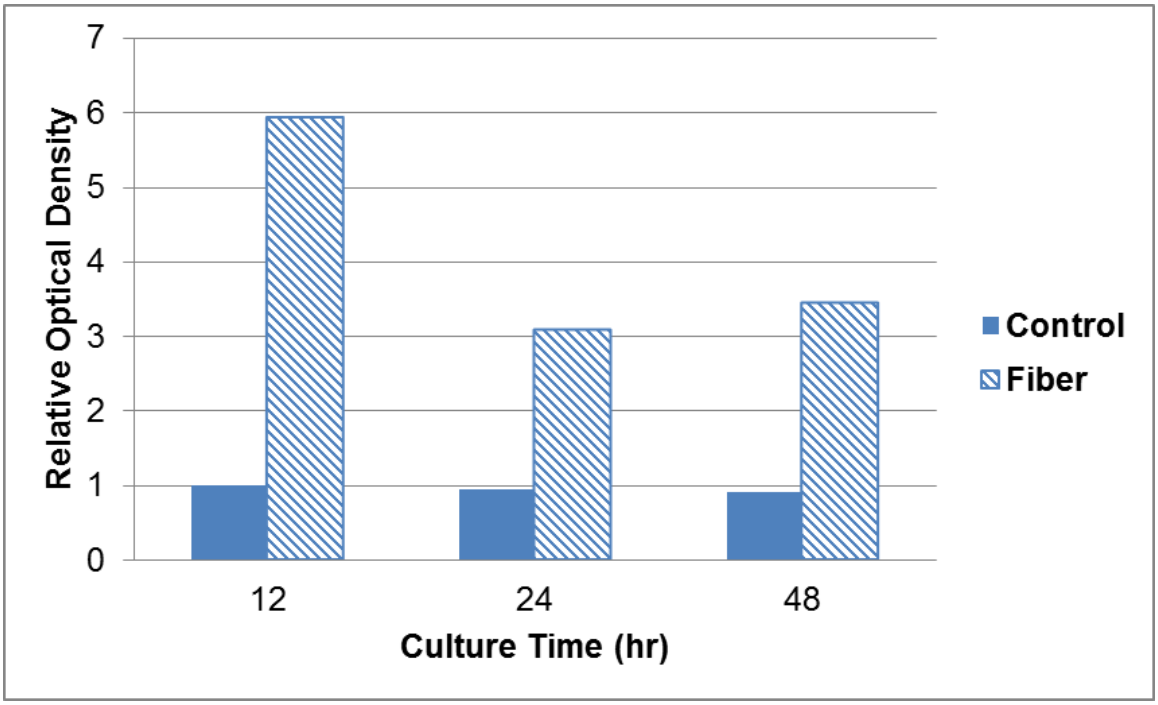

Figure 3.3.4 Relative optical density of RANKL for control and nanofiber substrates at 12, 24 and 48 time points. Optical densities were normalized to the 12 hour control.

The ratio of OPG to RANKL was calculated from the normalized OPG and RANKL data, as seen in Figure 3.3.4. The OPG/RANKL ratio is a good indicator of bone remodeling [10]; a low OPG/RANKL ratio indicates osteoclastic differentiation.

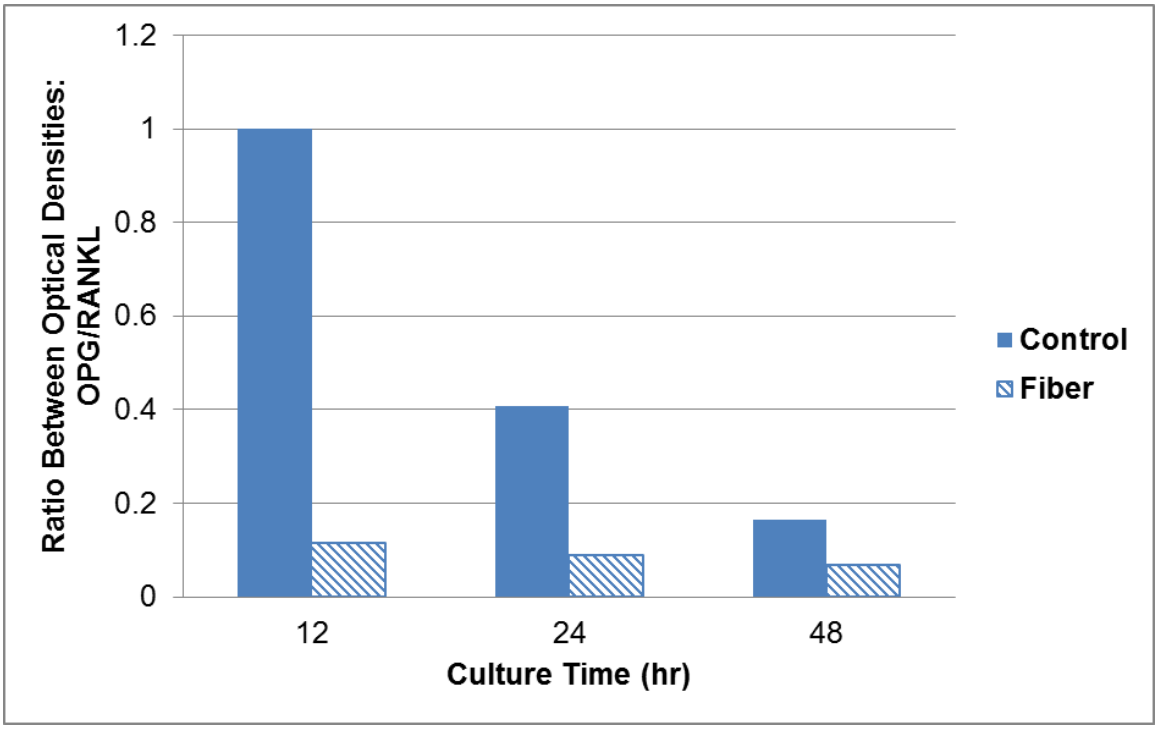

Figure 3.3.5 Normalized OPG/RANKL ratios.

3.3.2 Immunofluorescence assay results

M3CT3 cells on nanofiber substrates were stained for OPG and RANKL at 12, 24 and 48 hour time points. Fluorescence microscopy reveals localization of OPG and RANKL. In both control and nanofiber substrates at all three time points, OPG tends to be expressed across the entire cellular membrane while RANKL is more concentrated around the cell nucleus, as shown in Figure 3.3.6.

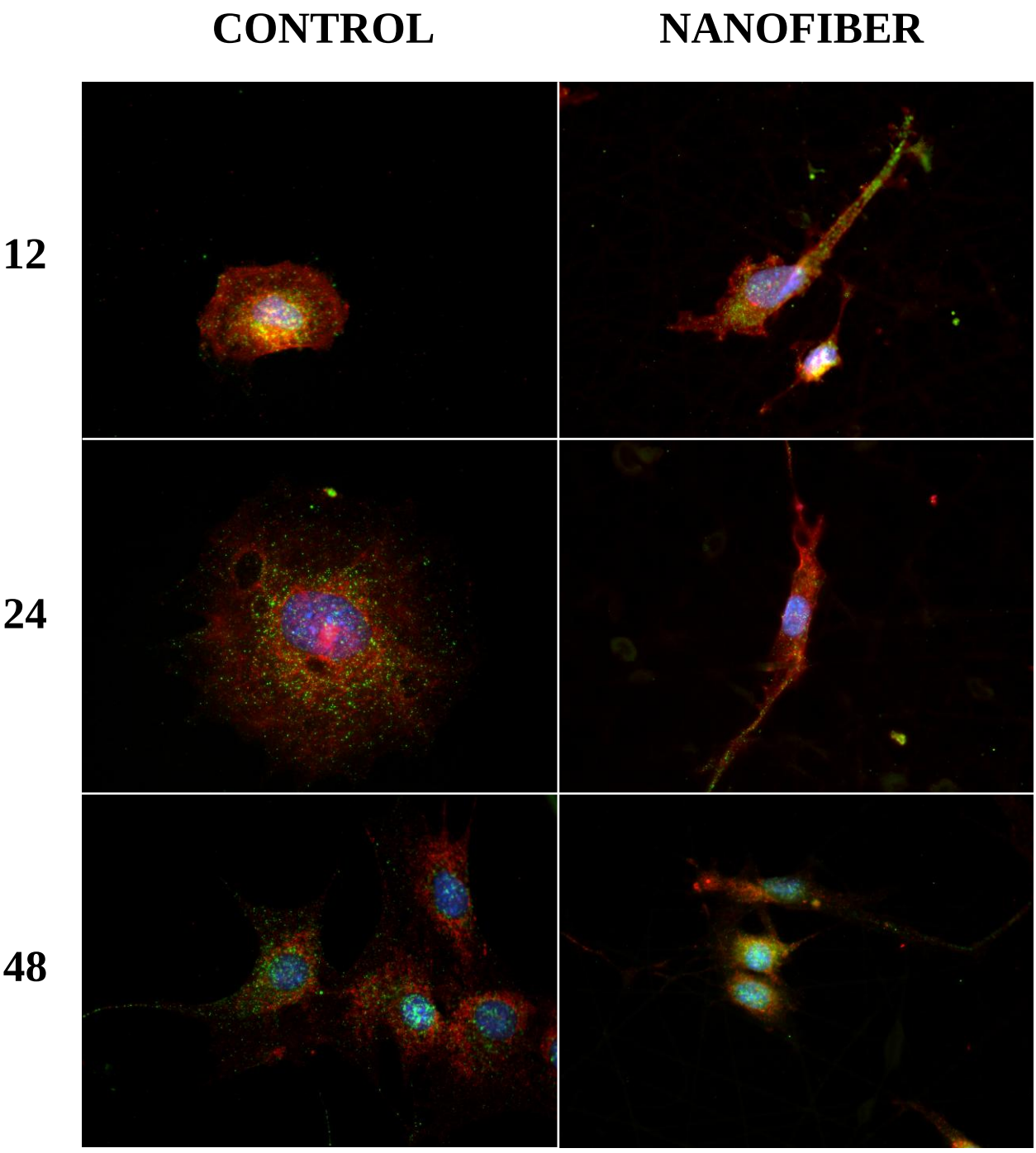

Figure 3.3.6 RANKL (green) and OPG (red) expression of a cell on control and nanofiber substrates after 12, 24 and 48 hours.

Further immunoassays on cells cultured for 24 hours on control and nanofiber substrates demonstrate similar results. Upon visual inspection, RANKL expression

appears to be concentrated around the cell nucleus, as illustrated in Figure 3.3.7. OPG continues to be expressed on the cell membrane as the cell membrane extends across the nanofibers.

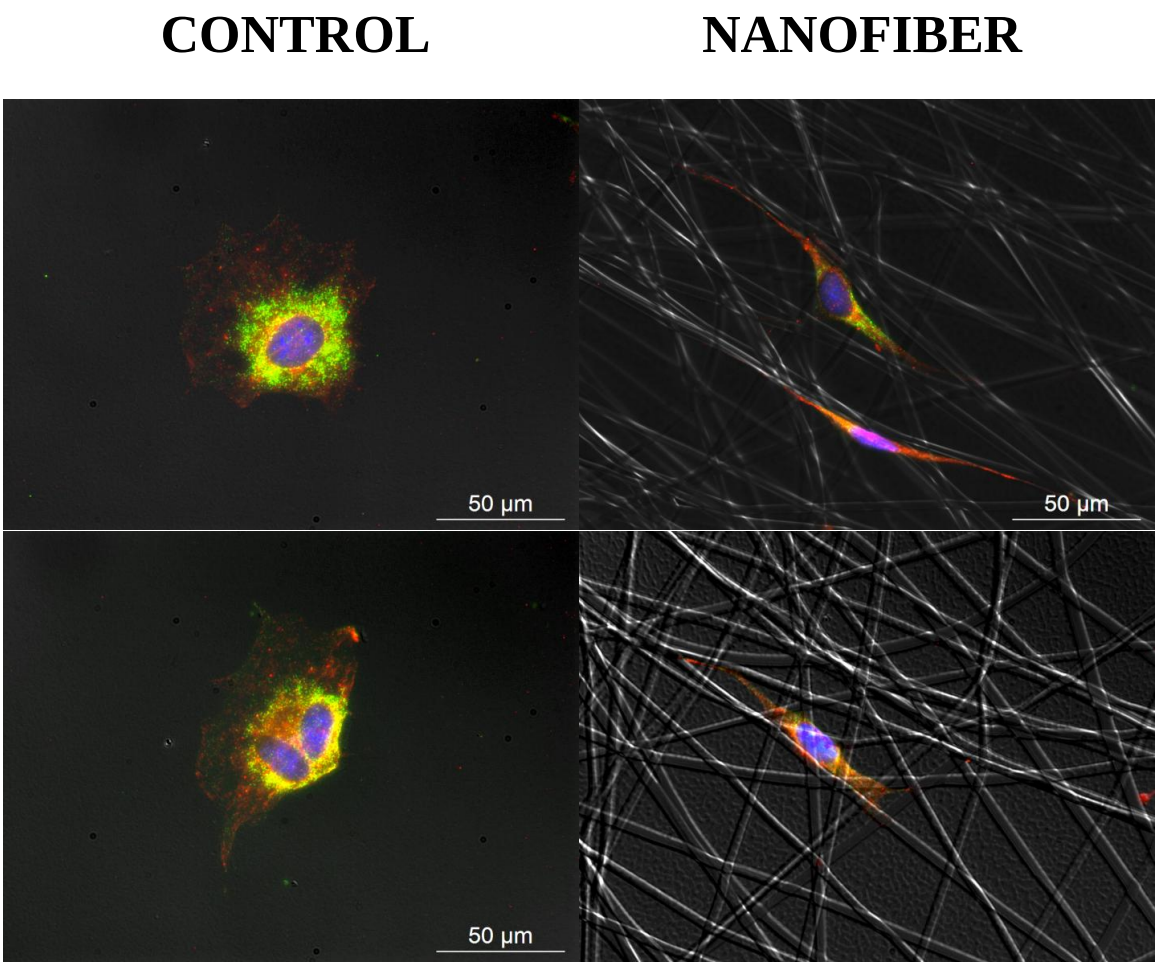

Figure 3.3.7 RANKL (green) and OPG (red) expression of a cell on control and nanofiber substrates after 24 hours.

3.4 Discussion

OPG concentration was found to decrease with time for both control and nanofiber substrates. Since OPG is the main protein responsible for the inhibition of osteoclastic demineralization, this suggests that the tendency for osteoclastogenesis decreases during the first

48 hours of culture. However, RANKL expression was also found to decrease for nanofiber substrates between the 12 and 24 hour time points. These findings are unexpected; although there are some contradictory data in literature, in general when OPG expression is down regulated, RANKL expression is up regulated [10]. In addition, we hypothesized that nanofiber substrates would promote osteoblastogenesis, so we expected a less RANKL expression for nanofiber substrates.

To further analyze this discrepancy, the ratio of OPG to RANKL was examined, as illustrated in Figure 3.3.5. The OPG/RANKL ratio decreased dramatically with time for control substrates but remained relatively constant for nanofiber substrates. The ratios for both substrates appear to be approaching the same value - a low OPG/RANKL ratio below 0.1. Ultimately, cells on both substrates move towards a phenotype that supports bone remodeling. However, cells on the nanofiber substrates appear to reach that state sooner than cells on the control substrates.

This trend may be due to an increase in Runx2 activity during the first 48 hours of culture. Osteoblastic differentiation from a stem cell to an osteoblast is promoted by the transcription factor Runx2; differentiation from an osteoblast to an osteocyte is inhibited by Runx2 [26]. The MC3T3 cells used in this experiment begin in a mesnchymal stem cell/osteoblast progenitor phase. Based on the OPG/RANKL ratios in Figure 3.3.5, it appears that the nanofiber substrates potentially promote the differentiation of the MC3T3 cells progenitor cells to osteoblasts faster than the control substrates, which only begin to differentiate after contact inhibition occurs. However, literature has shown that Runx2 expression decreases after additional time [27]. Therefore, RANKL expression is expected to increase for the control substrates and decrease on the nanofiber substrates at extended time points, as the MC3T3 cells begin to further differentiate into mature osteoblasts and osteocytes.

Results from immunofluorescence assays also shed light on the localization of OPG and RANKL. In both control and nanofiber substrates at all three time points, OPG is expressed along the entire cell membrane whereas RANKL tends to be expressed around the nucleus. These results agree well with literature [10]; since RANKL is typically a membrane-bound protein while OPG is a secreted protein, OPG can diffuse more readily than RANKL.

Chapter 4

MODULATING NANOFIBER DIAMETER AND DENSITY

4.1 Background on nanofiber modulation

Previous studies have indicated that nanofiber diameter cannot be regulated through needle size, but can be controlled by altering the percent composition of the polymer [18], [28] [25]. Lower weight percentages polymer will produce thinner nanofibers, while higher weight percentages will produce thicker nanofibers. However, the lower bound of nanofiber thickness is usually indicated by the formation of particles rather than fibers (electrospraying), while the upper bound is signaled by the onset of beading. The polymer concentration at each of these bounds varies between polymers.

On the other hand, the density of the deposited nanofibers can be regulated by changing the electrospinning time for each slide. Both low density and high density nanofiber films are expected to resemble a relatively "flat" substrate, whereas medium density nanofiber films will most readily exemplify true nanofiber architecture. In low density substrates, the PolyHEMA coated cover slip is predominately exposed. In high density substrates, the nanofibers completely cover the surface of the coverslip and form a homogeneous film.

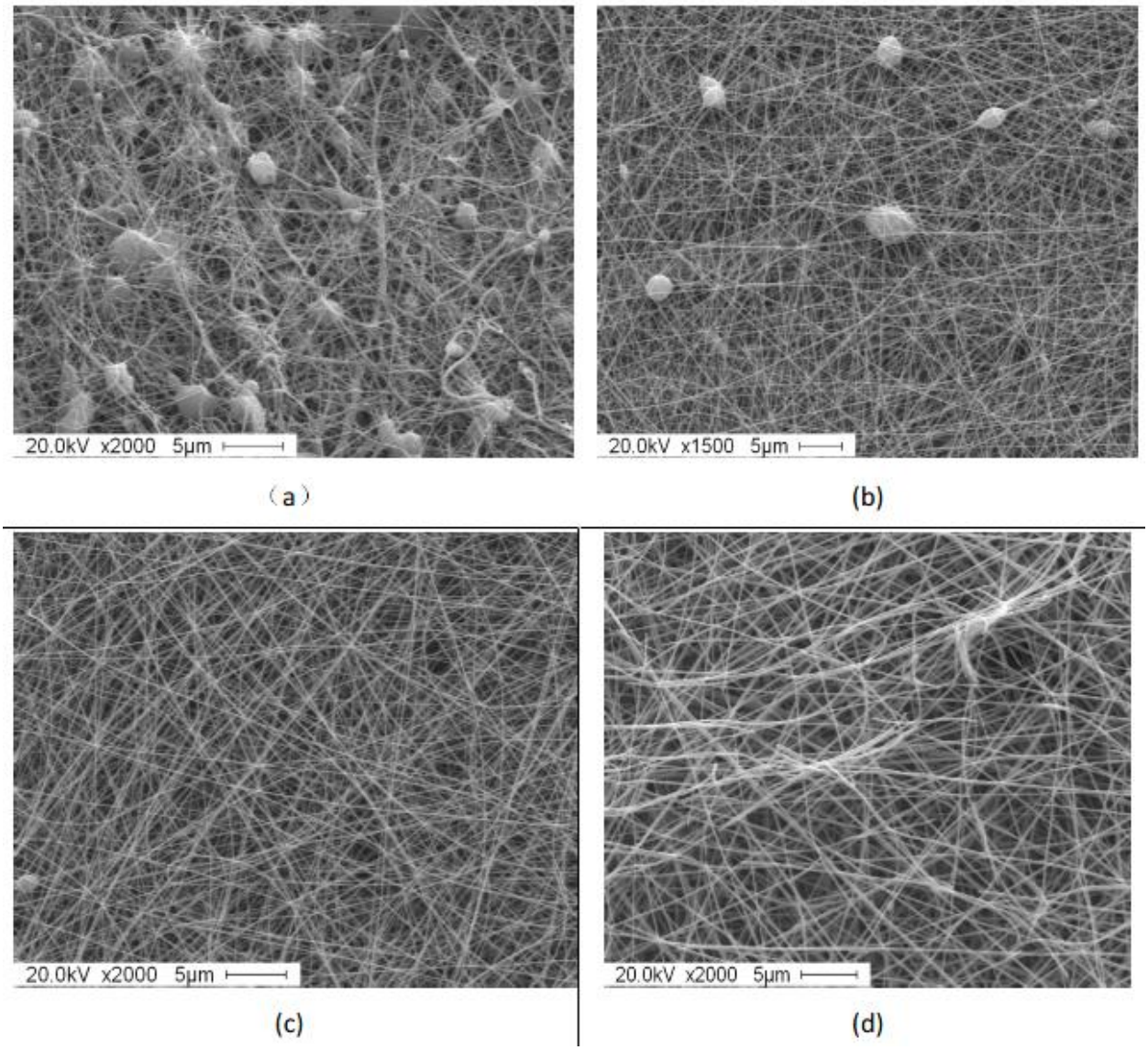

Figure 4.1.1 Morphology of polyacrylamide nanofibers at varying polymer concentrations [6].

Literature reveals successful modulation of nanofiber diameter for several polymers, including polyacrylamine, as seen in Figure 4.1.1. In this study, we seek to synthesize PMMA nanofibers of varying diameter and density. This will lead to future characterization of cellular phenotype progression on a range of nanofiber substrates. By observing the effects of nanofiber

diameter and density on the expression of OPG and RANKL, we can optimize nanofiber parameters for maximal mineralized matrix formation.

4.2 Experimental methods

4.2.1 Controlling nanofiber density

Six different nanofiber substrates were prepared from 25% PMMA in nitromethane (wt/vol), each having a different nanofiber density by varying the electrospinning time. Electrospinning times ranged from 10 to 60 in increments of 10 seconds. The control group was subjected to 20 seconds of electrospinning. Apart from altering the time for electrospinning, standard electrospinning procedure will be performed, as outlined in 3.2 Methods.

4.2.2 Controlling nanofiber diameter

Seven different polymer samples were prepared, each having a different ratio of PMMA to nitromethane (wt/vol). The concentrations ranged from 10-40% in increments of 5%. The control group comprised a 25% polymer concentration. Standard electrospinning procedure was performed, as outlined in 3.2 Methods. For polymer concentrations of 30-40%, the working solution was heated immediately prior to loading to decrease viscosity.

4.2.3 Assessing nanofiber diameter and density

Nanofiber substrates were imaged through bright field microscopy. Images were taken with a 20x dry objective and 40x wet objective. Nanofiber diameters and densities were determined using Image J software.

4.3 Results

4.3.1 Nanofiber density increases with electrospinning time

Nanofiber densities were found to increase with electrospinning time. Electrospun PMMA scaffolds appear as opaque white sheets. As seen in Figure 4.3.1, the nanofiber scaffold occupies a greater surface area of the cover slip for longer electrospinning times. At durations 20 seconds or less, uncoated areas on the cover slips remain visible. However, at durations 40 seconds or greater, the cover slip is completely covered in the nanofiber scaffold.

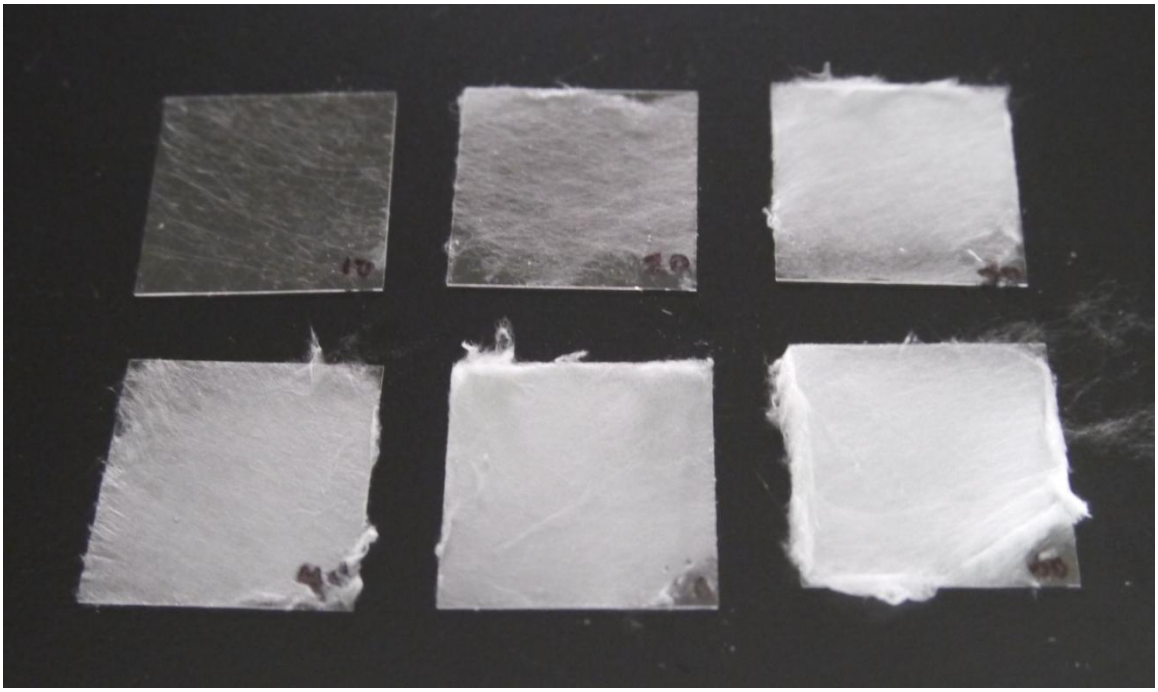

Figure 4.3.1. 25% PMMA nanofiber substrates at varying electrospinning durations. Top row left to right: 10, 20 and 30 seconds. Bottom row left to right: 40, 50 and 60 seconds.

These qualitative findings are further supported from bright field microscopy of the nanofibers. Figure 4.3.2 shows an increase nanofiber density with increasing electrospinning time. The electrospining apparatus continually deposits nanofibers on top

of each other to increase the scaffold thickness. Because of this, multiple planes of fibers will form during longer electrospinning times. This is clearly evident in scaffolds that were spun for 40, 50 and 60 seconds, in which unfocused fibers appear blurry.

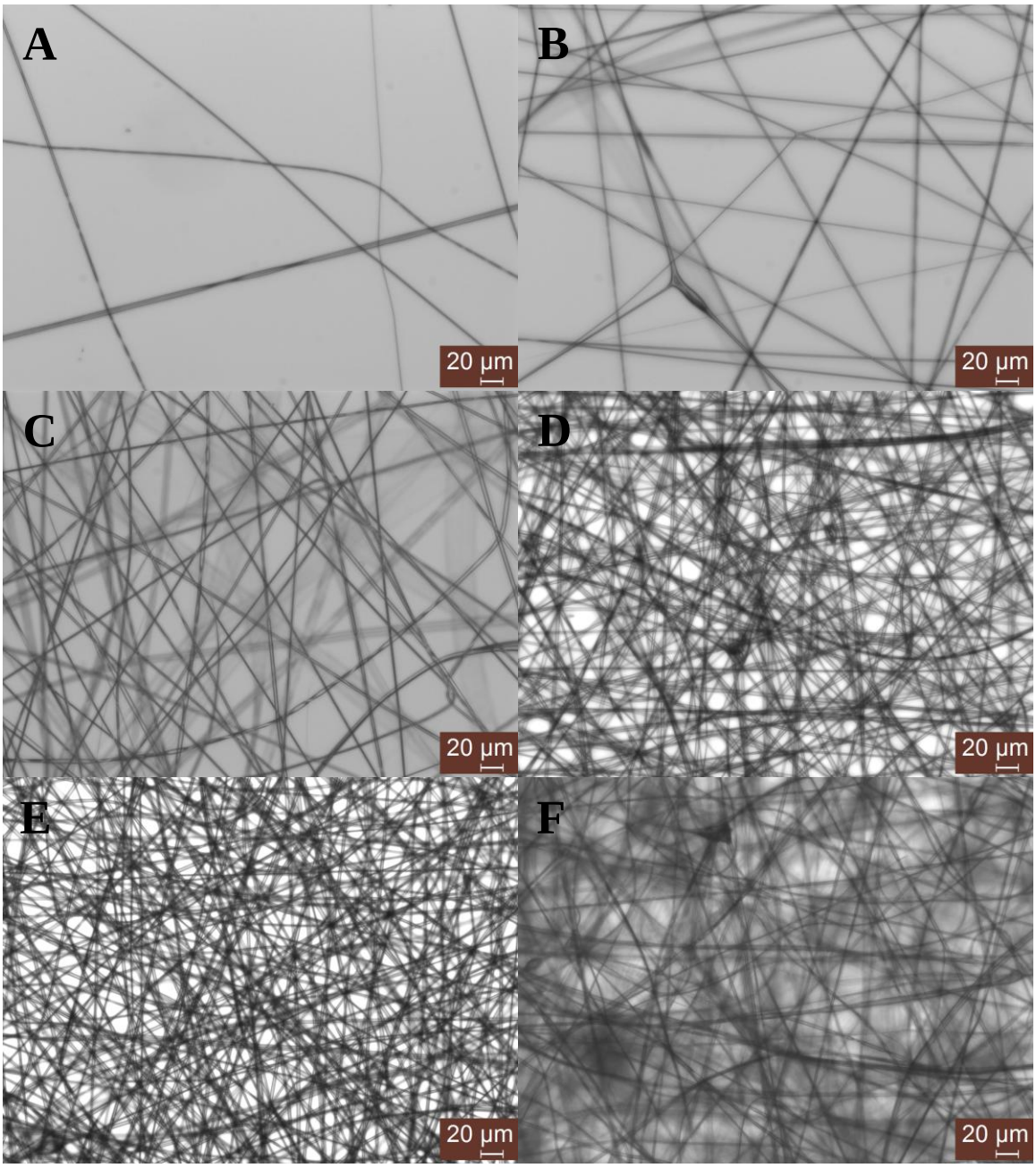

Figure 4.3.2. 25% PMMA nanofibers electrospun for 10, 20, 30, 40, 50 and 60 seconds (A-F, respectively) under a 20X dry objective. Light intensity was increased for D-E.

Nanofiber images were analyzed using ImageJ to calculate relative density. The relative area occupied by nanofibers on the cover slips was determined by applying a threshold. All areas occupied by nanofibers were redefined as black pixels and all areas not occupied by nanofibers were redefined as white pixels.

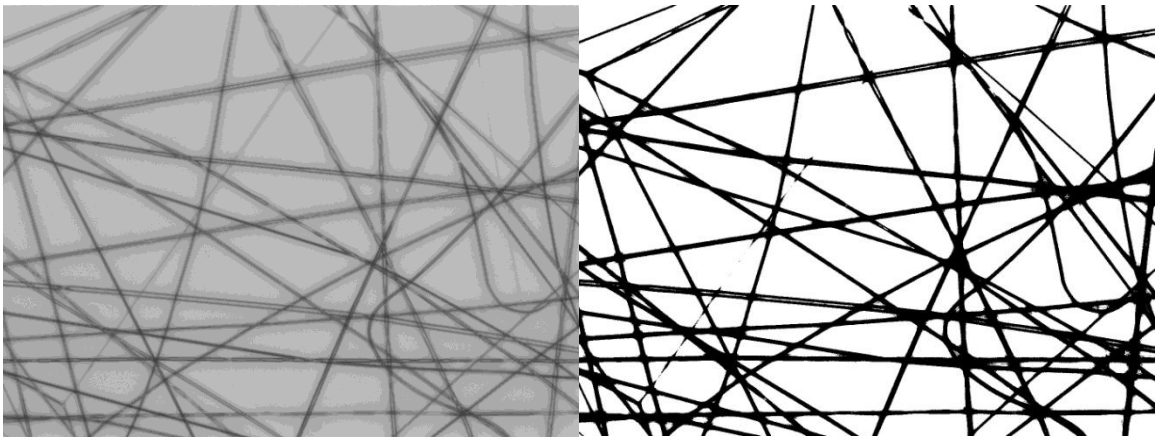

Figure 4.3.3. Image of a nanofiber substrate before (left) and after (right) threshold filter.

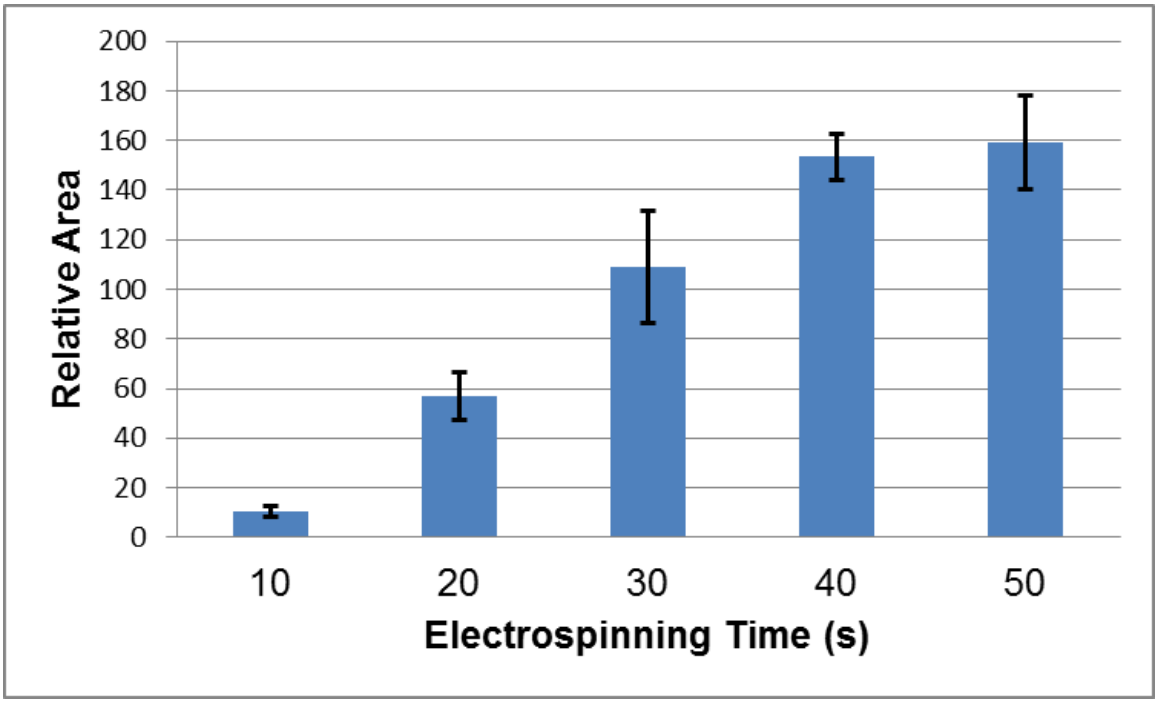

Figure 4.3.4. Relative area occupied black pixels after threshold application. The nanofiber substrate spun for 60 seconds was neglected because an accurate threshold could not be obtained due to unfocused fibers. Standard error means were used in the analysis with n=5.

After subjecting all images to a threshold filter, relative densities were found to increase with electrospinning time. Mean relative area appears to increase from 10-30 seconds then level off after 40 seconds.

4.3.2 Nanofiber diameter increases with polymer concentration

Upon visual inspection, nanofiber diameter appears to increase with increase in percent PMMA composition. Nanofiber density also appears to decrease at higher PMMA concentrations. In Figure 4.3.5, nanofibers spun from 10, 15 and 20% PMMA solutions exhibited heavy electrospraying. This is clearly evident in the 5-15µm beads uniformly distributed across the coverslip. Electrospraying did not occur for nanofibers spun from 25, 30, 35 and 40% PMMA solutions, as seen in Figure 4.3.6.

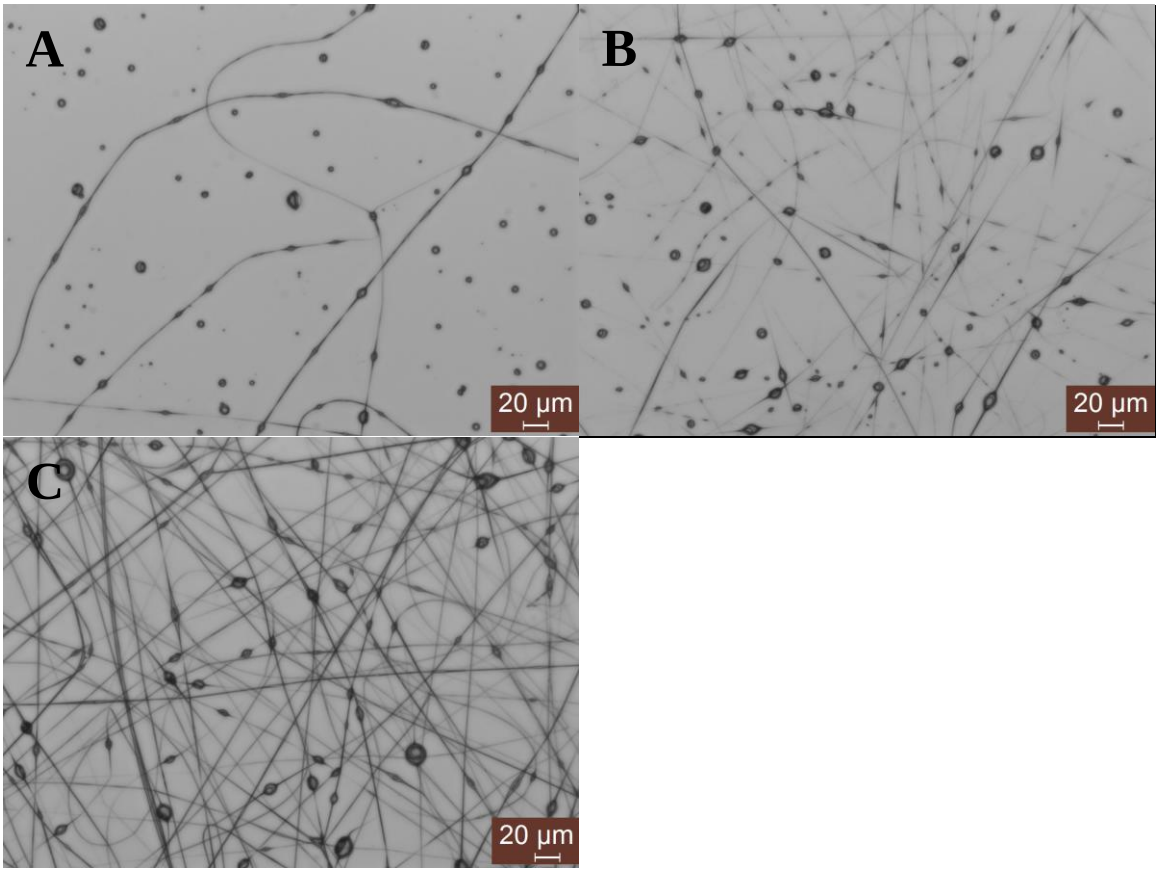

Figure 4.3.5. Electrospun nanofibers at 10% (A), 15% (B) and 20% (C) PMMA to nitromethane (wt/vol) concentrations. Images were taken using bright field microscopy at 20x magnification.

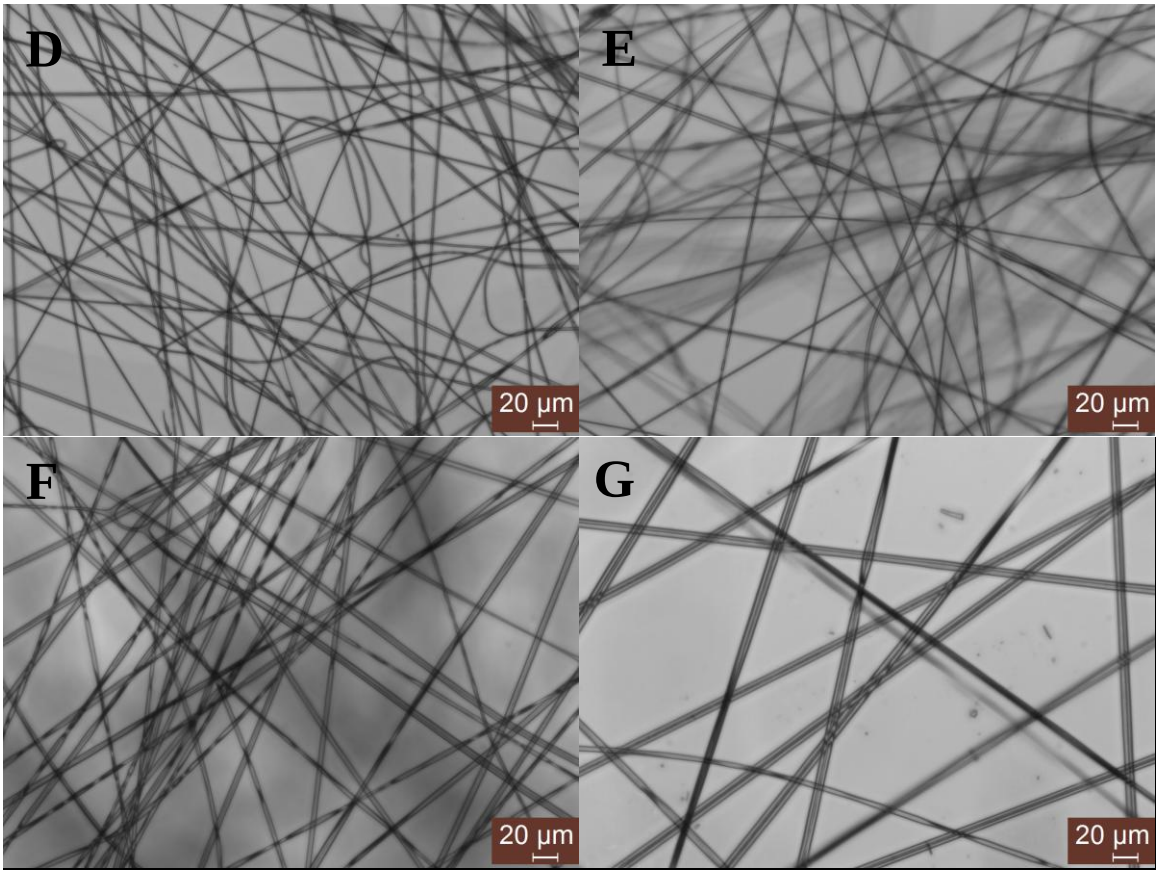

Figure 4.3.6. Electrospun nanofibers at 25% (D), 30% (E), 35% (F) and 40% (G) PMMA to nitromethane (wt/vol) concentrations. Images were taken using bright field microscopy at 20x magnification.

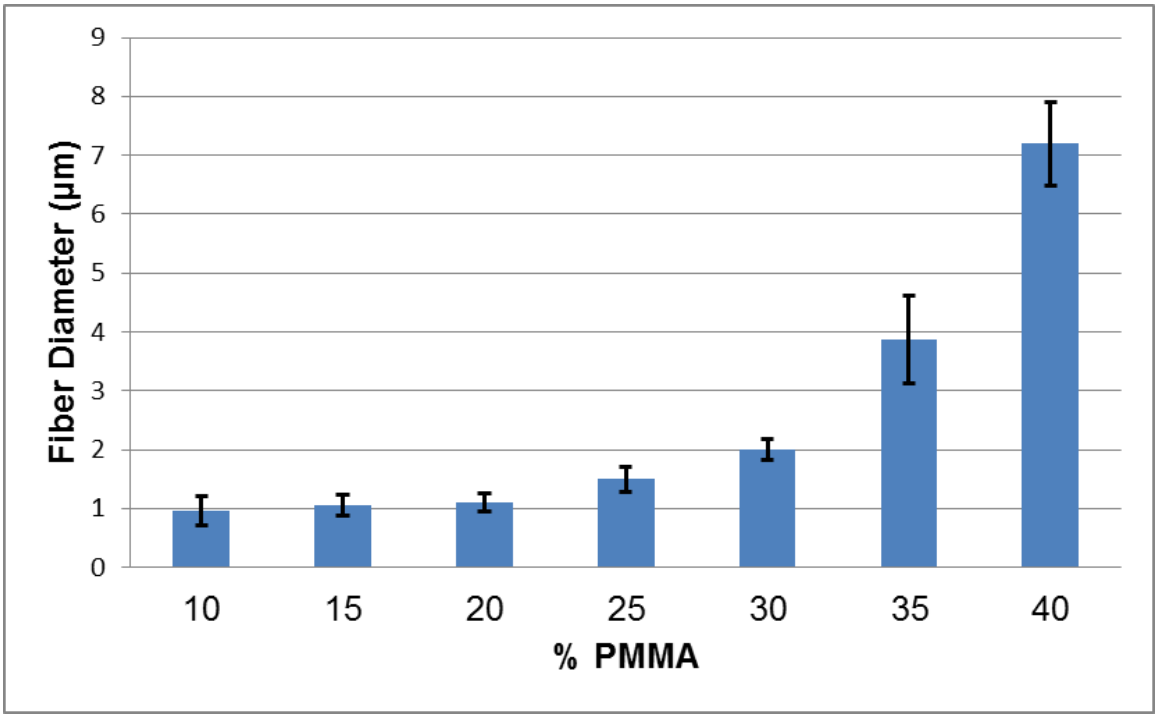

Figure 4.3.7 Nanofiber diameter at varying PMMA polymer concentrations. Standard error means were used in the analysis with n=50.

Nanofiber diameter was characterized using Image J. As shown in Figure 4.3.7, nanofiber diameter remains around 1µm for 10-20% PMMA solutions but appears to increase exponentially for 25-40% PMMA solutions.

4.4 Discussion

In this study, nanofiber density and diameter were modulated by varying the electrospinning time and PMMA polymer concentration, respectively. Nanofiber density was found to increase with higher PMMA concentrations through visual inspection. ImageJ analysis demonstrates that relative area occupied by nanofibers increases with electrospinning time, indicating that nanofiber density also increases with electrospinning time. In Figure 4.3.4, the mean area appears to increase linearly for the first 40 seconds, then tail off after 40 seconds. The tail may be due to the overlap of the nanofibers; once the surface of the cover slip is saturated

with nanofibers, the mean area will be at a maximum and additional nanofiber layers will not contribute to the number of black pixels. It is expected that the mean relative area, as determined through the proportion of black pixels, will asymptotically approach a maximum value as electrospinning time increases.

Although this method is not completely accurate (threshold values were qualitatively determined and not all thresholds represent areas occupied by the fibers), this method is effective in quantitatively characterizing the relative relationship between density and electrospinning time.

Nanofiber diameter was also found to increase with polymer concentration. In Figure 4.3.7, nanofiber diameter remains relatively constant for 10-20% PMMA concentrations, then increases exponentially for 25-30% PMMA concentrations. The small change in diameter from 10-20% can be explained by electrospraying. The low PMMA concentration solutions do not have sufficient cohesion to hold the polymer together during electrospinning, resulting in electrospraying. This suggests that until a critical amount of cohesion is reached, electrospraying will limit the volume of polymer jet forming the nanofibers. At a 25% PMMA concentration, electrospraying ceases and nanofiber diameter significantly increases, indicating that the critical cohesion is met. Increasing polymer cohesion by increasing the polymer concentration promotes the formation of thicker nanofibers. However, density is observed to decrease with increasing polymer concentration. Higher concentration polymer solutions (30-40% PMMA) do not jet as readily as lower concentration polymers due to high viscous forces. Therefore, for a given electrospinning time, lower concentration polymer solutions tend to generate a greater number of nanofibers than higher concentration polymer solutions.

By modulating the diameter and density of nanofibers, nanofibers can be optimized to promote maximum mineralized matrix formation. This study will lead to future characterization of OPG and RANKL on nanofiber substrates of varying diameter and density.

Chapter 5

CONCLUSIONS

5.1 Summary conclusions

In general, this thesis found that nanofiber architecture supports MC3T3 cell growth and may serve as a suitable substrate for bone tissue engineering applications. Nanofibers substrates were successfully synthesized from a 25% vol/vol PMMA solution using the electrospinning technique. MC3T3 cells were cultured on control and nanofiber substrates for 12, 24 and 48 hours. OPG and RANKL protein expression were quantitatively and qualitatively characterized through Western blotting and immunofluorescence assays, respectively. Finally, variations in the PMMA polymer concentration and electrospinning time were found to affect the nanofiber diameter and density, respectively.

To establish the viability of MC3T3 cells on PMMA nanofiber substrates, cells were cultured on nanofiber substrates for 12, 24 and 48 hours and stained for actin, a major cytoskeletal protein. Specific Aim 1 was achieved; fluorescence and SEM images demonstrated that cells successfully adhered to the nanofibers. In addition, cells on nanofibers tended to proliferate and migrate in the direction of the local nanofibers. Together with the porous nature and mechanical properties of the nanofiber scaffolds, this study indicates that PMMA nanofiber scaffolds may be a suitable substrate for bone cell growth.

This study also characterized the expression of OPG and RANKL, two integral membrane proteins in the NF-κB signaling pathway. Specific Aim 2 was achieved, since results revealed altered expression of OPG and RANKL between control and nanofiber substrates. OPG

and RANKL were found to be expressed along the cell membrane and around the cell nucleus, respectively. The ratio of OPG/RANKL was greater for control substrates compared to nanofiber substrates for all three time points. However, the ratio dramatically decreased for control substrates while remaining relatively constant for nanofiber substrates. The ratio for all substrates appeared to converge on a single value less than 0.1. This indicates that both substrates ultimately move cells toward the same pro-remodeling phenotype, but cells on the nanofiber substrates are able to reach a homeostatic state quicker. Although the OPG/RANKL ratio was lower for nanofiber substrates for the first 48 hours of culture, literature suggests that the ratio could increase for nanofiber substrates with additional time [27].

Furthermore, Specific Aim 3 was achieved. The diameters and densities of nanofibers were successfully modulated. Nanofiber diameters were controlled by changing polymer concentration, forming1-8μm thick nanofibers . Density was regulated through electrospinning time to create a range of varying density substrates. This study supports existing research on electrospun nanofiber modulation and sheds light on methods to regulate the thickness and density of PMMA nanofiber scaffolds.

Overall, this thesis demonstrates that PMMA nanofiber can be engineered to fit specific parameters through electrospinning. These nanofiber substrates promote bone differentiation and may induce mineralized matrix formation in the long term. Since the production of sufficient mineralized matrix remains one of the primary hurdles in bone tissue engineering, electrospun nanofibers may server as a suitable scaffold for bone tissue engineering applications.

5.2 Future work

The most important future steps would be to characterize the expression of OPG and RANKL under extended culture time to determine long-term trends and establish statistical significance. Based on literature data, it is expected that the OPG/RANKL expression ratio will increase for nanofiber substrates and decrease for control substrates with additional time after.

OPG and RANKL expression should also be characterized for nanofibers of varying diameter and density. By accessing the expression of these proteins, parameters for nanofiber diameter and density can be optimized for maximum osteoid matrix formation as indicated by a large OPG/RANKL ratio in the long term.

Finally, MC3T3 cells can be stained for cytoskeletal proteins such as FAK and vinculin, in addition to actin. Cell proliferation and migration on control and nanofiber substrates should also be captured through video. This will lead to a better understanding of cellular adhesion and movement on PMMA nanofiber substrates.

REFERENCES

[1] R. Langer and J. P. Vacanti, "Tissue Engineering," *Science*, vol. 260, pp. 920-926, 1993.

[2] H. Yoshimoto, Y. M. Shin, H. Terai, and J. P. Vacanti, "A biodegradable nanofiber scaffold by electrospinning and its potential for bone tissue engineering," *Biomaterials*, vol. 24, no. 12, pp. 2077-2082, May 2003.

[3] B. F. Boyce, Z. Yao, and L. Xing, "Functions of nuclear factor kappaB in bone.," *Annals of the New York Academy of Sciences*, vol. 1192, pp. 367-75, Mar. 2010.

[4] N. X. Chen, D. J. Geist, D. C. Genetos, F. M. Pavalko, and R. L. Duncan, "Fluid shear-induced NFκB translocation in osteoblasts is mediated by intracellular calcium release," *Bone*, vol. 33, no. 3, pp. 399-410, Sep. 2003.

[5] H. Tanaka, T. Mine, H. Ogasa, T. Taguchi, and C. T. Liang, "Expression of RANKL/OPG during bone remodeling in vivo.," *Biochemical and biophysical research communications*, vol. 411, no. 4, pp. 690-4, Aug. 2011.

[6] L. Liu, W. W. Gu, W. T. Xv, and C. F. Xiao, "Preparation of Polyacrylamide Nanofibers by Electrospinning," *Advanced Materials Research*, vol. 87-88, pp. 433-438, Dec. 2009.

[7] A. J. Salgado, O. P. Coutinho, and R. L. Reis, "Bone tissue engineering: state of the art and future trends.," *Macromolecular bioscience*, vol. 4, no. 8, pp. 743-65, Aug. 2004.

[8] M. Zaidi, "Skeletal remodeling in health and disease.," *Nature medicine*, vol. 13, no. 7, pp. 791-801, Jul. 2007.

[9] D. V. Novack, "Role of NF-κB in the skeleton.," *Cell research*, vol. 21, no. 1, pp. 169-82, Jan. 2011.

[10] S. Theoleyre, Y. Wittrant, S. K. Tat, Y. Fortun, F. Redini, and D. Heymann, "The molecular triad OPG/RANK/RANKL: involvement in the orchestration of pathophysiological bone remodeling.," *Cytokine & growth factor reviews*, vol. 15, no. 6, pp. 457-75, Dec. 2004.

[11] T. W. Bauer, "Bone graft substitutes.," *Skeletal radiology*, vol. 36, no. 12, pp. 1105-7, Dec. 2007.

[12] H. L. Morris, C. I. Reed, J. W. Haycock, and G. C. Reilly, "Mechanisms of fluid-flow-induced matrix production in bone tissue engineering," *Proceedings of the Institution of Mechanical Engineers, Part H: Journal of Engineering in Medicine*, vol. 224, no. 12, pp. 1509-1521, Dec. 2010.

[13] L. Nassif and M. El Sabban, "Mesenchymal Stem Cells in Combination with Scaffolds for Bone Tissue Engineering," *Materials*, vol. 4, no. 10, pp. 1793-1804, Oct. 2011.

[14] Y. Ito et al., “A composite of hydroxyapatite with electrospun biodegradable nanofibers as a tissue engineering material.,” *Journal of bioscience and bioengineering*, vol. 100, no. 1, pp. 43-9, Jul. 2005.

[15] J. Fang, H. Niu, T. Lin, and X. Wang, “Applications of electrospun nanofibers,” *Chinese Science Bulletin*, vol. 53, no. 15, pp. 2265-2286, Aug. 2008.

[16] G. Ma, D. Fang, Y. Liu, X. Zhu, and J. Nie, “Electrospun sodium alginate/poly(ethylene oxide) core–shell nanofibers scaffolds potential for tissue engineering applications,” *Carbohydrate Polymers*, vol. 87, no. 1, pp. 737-743, Jan. 2012.

[17] S. P. Nukavarapu et al., “Polyphosphazene/nano-hydroxyapatite composite microsphere scaffolds for bone tissue engineering.,” *Biomacromolecules*, vol. 9, no. 7, pp. 1818-25, Jul. 2008.

[18] H. Wang et al., “Electrospun poly(methyl methacrylate) nanofibers and microparticles,” *Journal of Materials Science*, vol. 45, no. 4, pp. 1032-1038, Nov. 2009.

[19] J. Xu et al., “NF-kappaB modulators in osteolytic bone diseases.,” *Cytokine & growth factor reviews*, vol. 20, no. 1, pp. 7-17, Feb. 2009.

[20] G. Martini et al., “Serum OPG and RANKL levels before and after intravenous bisphosphonate treatment in Paget’s disease of bone.,” *Bone*, vol. 40, no. 2, pp. 457-63, Feb. 2007.

[21] G. N. Belibasakis and N. Bostanci, “The RANKL-OPG system in clinical periodontology.,” *Journal of clinical periodontology*, vol. 39, no. 3, pp. 239-48, Mar. 2012.

[22] B. F. Boyce and L. Xing, “Functions of RANKL/RANK/OPG in bone modeling and remodeling.,” *Archives of biochemistry and biophysics*, vol. 473, no. 2, pp. 139-46, May 2008.

[23] M. M. Stevens and J. H. George, “Exploring and engineering the cell surface interface.,” *Science (New York, N.Y.)*, vol. 310, no. 5751, pp. 1135-8, Nov. 2005.

[24] K. T. Chu, Y. Oshida, E. B. Hancock, M. J. Kowolik, T. Barco, and S. L. Zunt, “Hydroxyapatite / PMMA composites as bone cements,” *Bio-medical Materials and Engineering*, vol. 14, pp. 87-105, 2004.

[25] S. Piperno, L. Lozzi, R. Rastelli, M. Passacantando, and S. Santucci, “PMMA nanofibers production by electrospinning,” *Applied Surface Science*, vol. 252, no. 15, pp. 5583-5586, May 2006.

[26] H. Enomoto et al., “Induction of osteoclast differentiation by Runx2 through receptor activator of nuclear factor-kappa B ligand (RANKL) and osteoprotegerin regulation and

partial rescue of osteoclastogenesis in Runx2-/- mice by RANKL transgene.," *The Journal of biological chemistry*, vol. 278, no. 26, pp. 23971-7, Jun. 2003.

[27] J. L. Brown, M. S. Peach, L. S. Nair, S. G. Kumbar, and C. T. Laurencin, "Composite scaffolds: bridging nanofiber and microsphere architectures to improve bioactivity of mechanically competent constructs.," *Journal of biomedical materials research. Part A*, vol. 95, no. 4, pp. 1150-8, Dec. 2010.

[28] J. Macossay, A. Marruffo, R. Rincon, T. Eubanks, and A. Kuang, "Effect of needle diameter on nanofiber diameter and thermal properties of electrospun poly (methyl methacrylate)," *Polymers for Advanced Technologies*, no. February, pp. 180-183, 2007.

Permanent Address
503 Francis Drive
Mechanicsburg, PA 17050

Christopher Hong

cxh5051@psu.edu
(717) 418-5269

Current Address
127 North Sparks Street #1
State College, PA 16801

Education and Academics

University Park, PA **The Pennsylvania State University, College of Engineering, Schreyer Honors College**
Bachelor of Science in Bioengineering with Honors, Expected May 2012

Undergraduate Thesis: "The role of nanofiber architecture in NFκB signaling"

Awards and Honors: New York Times Public Speaking Contest nominee (2011), Penn State Summer Discovery Grant (2011), Hartz Scholarship in Engineering (2011) Engineering Excellence Scholarship (2010), NIST Undergraduate Research Fellowship (2009), Best Engineered Design Award by People's Choice (2009), NASA Pennsylvania Space Grant (2008)

University Research Experience

University Park, PA **The Pennsylvania State University,** Department of Bioengineering **1/2011-Present**
Honors Undergraduate Researcher (40 hours/week for summer, 6 hours/week during school)
- Investigated the role and regulation of NFκB growth factor in bone tissue proliferation
- Designed and conducted Western blot and immunofluorescence assays
- Presented findings at the 2011 Biomedical Engineering Society national conference
- Applied technical writing experience to obtain research funding through grant proposals

University Park, PA **The Pennsylvania State University**, Department of Animal Science **1/2010-12/2010**
Undergraduate Researcher (6 hours/week)
- Contributed to the launch of a new tissue engineering/regenerative medicine lab
- Learned cell culture techniques to study the regulation of ID4 gene in mouse ESC's

Work Experience

University Park, PA **The Pennsylvania State University**, Department of Biology **8/2010-Present**
Teaching Assistant (9 hours/week)
- Served as the sole instructor for multiple physiology lab sections with responsibilities of delivering lectures, leading *ex vivo* dissection experiments and reinforcing course material
- Collaborated with fellow teaching assistance to develop effective class exercises
- Maintained effective communication and relations between course supervisors and students

Skillman, NJ **Johnson & Johnson Consumer and Personal Products Worldwide**, **5/2010-8/2010**
Oral Health Care Research & Development
Research Intern (40 hours/week)
- Explored novel enamel imaging techniques for new Listerine mouthwash claims generation
- Analyzed FDA guidelines for medical devices to develop appropriate experiment protocols
- Communicated research to co-workers and supervisors through oral presentations and poster symposiums

Gaithersburg, MD **National Institute of Standards and Technology**, **5/2009-8/2009**
Center for Nanoscale Science and Technology
Research Fellow (40 hours/week)
- Worked closely with the principle investigator and research team to engineering and fabricate a nanoscale biosensor prototype
- Drafted abstracts and shared discoveries with fellow scientists through oral presentations

Laboratory Skills

Cell culture, Western blot assay, immunofluorescence assay, polymerase chain reaction, gel electrophoresis, confocal and fluorescence microscopy, electron microscopy/lithography, nanofabrication, ISO 5 cleanroom operations

Professional Organizations and Service

State College, PA **Mount Nittany Medical Center**, Volunteer **6/2011-Present**
University Park, PA **Biomedical Engineering Society**, Treasurer **8/2009-Present**
University Park, PA **Engineering House**, Treasurer and Mentor **8/2009-5/2011**